

# Revision of Quark Charge Calculations Using Supersymmetry (SUSY) Inversion Framework and Resolution of Baryon Asymmetry

Keryn Johnson<sup>1,\*</sup> and Amal Pushp<sup>2</sup>

<sup>1</sup> Quantum Technologies Ltd , 39a Bombay Street, Ngaio, Wellington 6035, New Zealand

<sup>2</sup> Department of Physics, Birla Institute of Technology, Mesra, Ranchi 835215, India

Received: 9 Nov. 2024, Revised: 3 Jan. 2025, Accepted: 19 Feb. 2025.

Published online: 1 Apr. 2025

**Abstract:** This paper presents a novel approach to quark charge calculations that revises the conventional atomic model by identifying the presence of antimatter, specifically positrons, within neutrons. In this revised framework, the neutron is no longer electrically neutral but instead is composed of a negatively charged core balanced by a positively charged positron. This redefinition introduces a Boson-like quark structure and establishes baryonic symmetry, allowing for the creation of matter and antimatter in equal quantities. Such symmetry addresses the long-standing problem of missing antimatter in cosmology. The inclusion of positrons in atomic structures not only restores charge parity but also provides a foundation for applying supersymmetry (SUSY) principles in biological systems. Unlike the traditional atomic model, which considers only protons, neutrons, and electrons, this new framework supports a symmetrical and unified representation of atomic and biological processes. The SUSY inversion quark charge model thus opens the possibility for exploring quantum coherence, charge conservation, and matter-antimatter interactions across disciplines, from fundamental physics to quantum biology.

**Keywords:** Baryonic symmetry, quark charge, He-BEC singularity, dark energy, dark matter, quantum gravity, cosmology.

## 1 Introduction

The Standard Model of particle physics assigns fractional quark charges (Up:  $+ \frac{2}{3}$ , Down:  $- \frac{1}{3}$ ), yielding proton (+1) and neutron (0) charges through additive calculations [1, 2]. Despite its successes, it fails to address the cosmological missing antimatter problem, the nature of dark energy (68%) and dark matter (27%) [3], and the unification of quantum mechanics (QM) with general relativity (GR). Observations from the James Webb Space Telescope (JWST) reveal young, bright galaxies, challenging the hot Big Bang model's timeline [4]. The cosmic microwave background's (CMB) homogeneity and the horizon problem further necessitate alternative frameworks [5].

This paper proposes the Supersymmetry (SUSY) inversion quark charge calculation model, using whole-number charges (Up: -1, Down: +1) and multiplicative operations to establish a negatively charged neutron (-1) balanced by a positron (+1). The new SUSY inversion quark charge calculation could enable the discovery of positrons present in the neutrons of the atom's nucleus. Alternatively, identify the positron within the orbital dynamics of an atom. The beta minus decay of the neutron into a proton and an electron, and an antineutrino, with a half-life of 888 seconds for the free neutron's down quark, is thus explained by the presence of the positron (half-life of 75 seconds) associated with the neutron through entanglement.

In contrast, the decay of a free proton has not been observed. The proton is currently considered to be stable in comparison to the free neutron's instability. This difference in stability can be accounted for by the energy and charge balance within the structure of the proton where  $2.2 \times 2.2 = 4.84$  ( $uu = d$ ) and  $-1 \times -1 = +1$ , whereas ( $dd \neq u$ ) and  $(+1 \times +1 = +1)$ . The neutron is known to have a larger mass than the proton despite both having three quarks. The Down quark  $4.84 \times 10^6 \text{ eV}/c^2$  is slightly heavier than the Up quark  $2.2 \times 10^6 \text{ eV}/c^2$ . The absence of charge on the neutron is accounted for in the new SUSY inversion model by its inclusion of a positron, where  $(+1 - 1 = 0)$ .

The SUSY inversion quark charge calculation for the neutron generates an overall charge of negative one (-1) and accounts for the attraction between the proton (+1) and neutron (-1) in the nucleus of atoms, giving rise to the Strong force. The SUSY inversion quark charge calculations reveal Baryonic symmetry, resolving the antimatter deficit. Integrated within the Helium Bose-Einstein Condensate (He-BEC) isotropic singularity framework, the model posits the universe was generated from a superfluid helium-4 initial state with zero charge and mass. The emission of neutral alpha particles from the helium Bose Einstein condensate is proposed to be responsible for the formation of dark energy and dark matter. The emission of alpha particles initiated cosmic inflation, where energy conservation processes balance the flow of energy between dark energy and dark matter. The outward cosmic inflation

\*Corresponding author e-mail: [k.johnson@ohbeehave007.com](mailto:k.johnson@ohbeehave007.com)

(red shift) mediated by dark energy and the inward dark matter implosion to generate cosmic compression (blue shift). Conservation rules maintaining the initial energy level of the He-BEC isotropic singularity.

The framework also predicts the universe's composition after 13.8 billion years and unifies QM and GR through inverse square law mathematics within the geometric constraints of a molecular structure. This addresses the role of beta decay, electromagnetic interactions, and transformation of light into atomic form and has biological implications linked to a biological mechanism operational in consciousness. In this paper, we will focus our attention on presenting the revised quark charge calculations based on the SUSY inversion model and some of its implications. The rest will hopefully be presented elsewhere in a follow-up papers.

## 2 Background and Motivation

### 2.1 The Quark Model and Relevance in Biology

The quark model was proposed independently by Gell-Mann, and Zweig (1964). Biology has focused on the hadrons (proton and neutron) and has not considered quarks and their charges and the implications other than considering that a proton has a charge of plus one and the neutron has no charge. Biology has focused its attention on the chemistry of biological systems, which has primarily focused on the electron and its role in bonding and molecular interactions, mitochondrial electron transport in ATP generation, as the energy currency of cellular metabolism.

Physics on the other hand, has three generations of quarks, also known as six flavours (June, 2008). Physics also has three generations of electrons, each with a heavier mass than the electron that biology focuses on. The roles of the heavier quarks and electrons is completely ignored by biologists. The first generation and the heaviest is the Tau particle -1, with its Bottom  $-1/3$ , and Top  $+2/3$  quarks; the muon particle -1, with its Charmed  $+2/3$ , and Strange  $-1/3$  quarks; and the electron particle -1 with its Up  $+2/3$ , and Down  $-1/3$  quarks (Nave., 2008).

Quarks are found in hadrons, which are found in the nucleus of atoms and include the proton and the neutron. There are three quarks in each hadron, but recently hadrons with more than three quarks have also been identified. The complexity of the zoo of particles that have been discovered by physicists within the nucleus of atoms has not previously been considered by biologists. As such, biology has a very simple atomic model that fails to understand the functional role the nucleus of the atom plays in biological processes. If one considers the origin of the 64 codon triplets and their coding redundancy in the coding of amino acids a possible explanation points to the three generations of Leptons and their quarks. Here,  $4^3 = 64$ . The three generations having a triplet orientation with the proton containing the three quarks UDU having a redundant U in the third position for quantum error correction and within the neutron DUD having a redundant D in the third position for quantum error

correction. Seen in this light, the three layers within quark theory correspond to the three letters of the codon sequence, which are timed through their half-lives. The fastest going first and slowest last. The Up and Down quarks having the longest half-lives provides the quantum error correction through low energy nuclear reactions (LENR) mediated by beta plus and beta minus decay processes.

An important analogy can be drawn from cell biology where the genes within the nucleus of a cell are expressed to give the functional proteins operating within the cellular environment. The nucleus expression system within the atom can be seen to be playing a functional role to transform the atomic landscape of the atom but its expression appears to be mediated through a theory that has not been understood in biology but has its basis in unstable atom theory. The physics of the three generations of quarks operating within the nucleus along with the heavier forms of the electron provide the basis of an atomic expression system that changes the functional properties of the atom that is produced because of the functional decay process mediated by W and Z Bosons. Chiral features of subatomic systems may be responsible for determining the biological molecule's chiral structure. This suggests that the origin of handedness is associated with beta decay processes within isotope physics. The subatomic angular momentum of the magnetic field rotation due to its surface charge properties and rotation orientation within the magnetic field, provides the basis for identifying the subatomic geometric structures operating within the atom that give rise to its chiral form. Biology needs answers to questions that cannot be obtained by remaining bound to the veneer of stable atoms. Deeper insight into the subatomic structure and function of atoms therefore may offer biologists a rationale as to the origin of life questions and resolve the chicken and egg issues associated with restricting evolution to mutational changes in DNA structure through the ideas of random point mutations. Directed evolutionary models are required to explain environmental selective pressure on an atomic scale.

### 2.2 Cosmological Challenges

The hot Big Bang assumes a 1D singularity at the Planck epoch ( $1.616 \times 10^{-35}$  m and  $5.39 \times 10^{-44}$  s), expanding via inflation at  $1 \times 10^{-36}$  s over  $1 \times 10^{27}$  m [4]. It predicts 5% matter, 27% dark matter, and 68% dark energy, but cannot identify their origins [3]. The CMB's uniformity and alternative theories (e.g., string theory, MOND) highlight unresolved issues [5].

### 2.3 Helium-4 and Bose-Einstein Condensates

Helium-4 exhibits superfluidity below 2.177 K, behaving as a Bose-Einstein Condensate (BEC) where electrons form a coherent wavefunction [7], a single wavelength. This makes Helium-4 a candidate for the universe's initial state, resolving CMB homogeneity and antimatter issues [8]. The He-BEC isotropic singularity model provides an initial radius of  $r = c$  and an alpha particle emission velocity of  $2.9907 \times 10^9$  m s $^{-1}$  along with a half-life of  $1 \times 10^{18}$  s, and an initial ground state wavelength of  $4 \times 10^{-14}$  m. A coherent

singularity that is large and uniform. Due to its uniform and homogeneous nature, a large 3-dimensional structure is proposed rather than the current 1D Big Bang model. Such an approach resolves the horizon problem in cosmology. The inability to detect dark energy and dark matter is resolved through this modelling approach. The conversion of an internal initial wavelength into a velocity provides an approach to utilize the initial state as a reference frame for the transformation taken place. Recently, it has been recognized that dark energy decreases over time. The features of the He-BEC alpha particle emission are associated with the decay of dark energy, which reduces over time due to the alpha particle half-life. The He-BEC model is aligned with the recent cosmological discoveries.

#### 2.4 Re-examining Fundamental Charge: Electron Dynamics and Quark Symmetry

The fundamental nature of how electrons carry charge remains incompletely explained within both the Standard Model and quantum mechanical frameworks, prompting deeper questions about the origin and essence of charge itself. When a proton and an electron form a bound system through entanglement, their charges cancel to produce net neutrality ( $q = +e + (-e) = 0$ ), superficially resembling a neutron's neutral state. However, their underlying quark compositions differ fundamentally—protons consist of two up quarks and one down quark (uud), while neutrons contain one up and two down quarks (udd), with the mass difference between up ( $\sim 2.2 \text{ MeV/c}^2$ ) and down ( $\sim 4.84 \text{ MeV/c}^2$ ) quarks preserving their distinct identities. Quantum chromodynamics (QCD) governs quark interactions through color charge mediated by massless gluons and mesons, operating independently from the electron's electromagnetic charge in atomic orbitals. Notably, the proton-neutron system exhibits an inverted quark symmetry, suggesting an underlying supersymmetric relationship. This observation has motivated an alternative inverted supersymmetry model for quark charge calculations, which reinterprets the elementary charge unit ( $e = 1.602 \times 10^{-19} \text{ C}$ ) through novel geometric considerations. The model proposes that electron charge manifestation may arise from an inverted surface charge density distributions ( $\int \rho_e(r) dV$ ) or surface charge phenomena. By attempting to identify elementary charge through the revision of quark charge calculations where  $uu = d$  and  $d(888 \text{ s}) = uu$ , the proton containing udu can be seen to contain  $u^4$  and despite the overall charge being +1, its internal quark charges adds to give -1 (see below) that offers a neutral system when considering an internal charge distribution giving +1 when multiplied (proton) + -1 (internal quark charges when summed together) = 0. A free proton, which is stable, may be positively charged from an external perspective but within the nucleus of individual quark charges summed together provide -1, overall, it observes a charge of 0 in the free state without the bound electron. The proposed model is revealing the whole atoms involvement in its charge properties and rather than charge being an arbitrary feature, it is part of the subatomic structure of the atom and can be used diagnostically to probe subatomic systems involved in charge formation.

#### 2.5 He-BEC charge calculations

The He-BEC model of charge via reciprocal energy conservation processes provides a whole-system-based set of calculations for the initial wavelength of  $4 \times 10^{-14} \text{ m}$  and the end wavelength of  $1.6 \times 10^{-35} \text{ m}$  (Planck). The He-BEC model postulates that the Planck distance is formed after cosmic inflation and is not present prior to this process taking place.

$$4 \times 10^{-14} \text{ m} / 1.6 \times 10^{-35} \text{ m} = 4 \times 10^{-22} \text{ m} \quad (1)$$

The difference between these two wavelengths corresponds to  $4 \times 10^{-22} \text{ m}$ . And this difference and its relationship to the initial reference frame of  $4 \times 10^{-14} \text{ m}$  is given by the following calculation.

$$4 \times 10^{-14} \text{ m} / 4 \times 10^{-22} \text{ m} = 1 \times 10^8 \text{ m} \quad (2)$$

where the point of balance is identified by its square root

$$(1 \times 10^8)^{0.5} = 1 \times 10^4 \quad (3)$$

And

$$1 \times 10^4 \text{ m} \times 4 \times 10^{-22} \text{ m} = 4 \times 10^{-18} \text{ m} \quad (4)$$

And

$$(4 \times 10^{-18})^{0.5} = 2 \times 10^{-9} \text{ m} \quad (5)$$

Which provides the surface area charge radius of

$$2 \times 10^{-9} \text{ m} / 4 \times 10^{-18} \text{ m} = 5 \times 10^8 \quad (6)$$

This correlates with the electric field from Planck

$$(1.6 \times 10^{-35})^{0.5} = 4 \times 10^{-18} \quad (7)$$

And the magnetic field from Planck.

$$(1.6 \times 10^{-35})^{0.25} = 2 \times 10^{-9} \quad (8)$$

The interaction between the electric and magnetic fields occurs through their multiplication given by the calculation.

$$2 \times 10^{-9} \text{ m} \times 4 \times 10^{-18} \text{ m} = 8 \times 10^{-27} \text{ m}^2 \quad (9)$$

This is aligned with the He-BEC gravitational implosion process from  $4 \times 10^{-14} \text{ m}$  to  $1.6 \times 10^{-35} \text{ m}$ , acting like the bookends on a shelf keeping the books upright and ordered. This suggests that the process of charge formation is directly determined by the initial structure of the singularity at the beginning of time prior to alpha particle emission and this is determined by its internal wavelength.

$$8 \times 10^{-27} \text{ m} / 1.6 \times 10^{-35} \text{ m} = 5 \times 10^8 \quad (10)$$

And

$$4 \times 10^{-18} \text{ m} / 8 \times 10^{-27} \text{ m} = 5 \times 10^8 \quad (11)$$

And

$$(5 \times 10^8)^4 \text{ m} = 6.25 \times 10^{34} \text{ m}^{-1} \left( \frac{1}{h} \right) \quad (12)$$

The charge surface area calculation corresponds to

$$(5 \times 10^8)^2 \text{ m} \times \pi \times 4 = 3.14 \times 10^{18} \text{ m}^2 \quad (13)$$

And its reciprocal,

$$\frac{1}{3.14 \times 10^{18}} = 3.18 \times 10^{-19} \text{ Coulombs} \quad (14)$$

This corresponds to  $2 \times$  elementary charge.

$$3.18 \times 10^{-19} / 2 = 1.59 \times 10^{-19} C \quad (15)$$

The location of the charge boundary membrane separating both positive (convex) and negative (concave) charges is proposed to be associated with the Charm quark and the Strange quark as the  $n=1$  in hydrogen barrier separation at  $5.7 \times 10^{27}$  Planck lengths corresponds to 137 (1/0.00729).

Matter antimatter annihilation is proposed to be associated with two gamma ray photons generation linked to positron and electron elementary charge. The distance between Planck  $1.6 \times 10^{-35}$  m and cosmic microwave background (CMB)  $1.6 \times 10^{-3}$  m is  $1 \times 10^{32}$  m, where the elementary charge is a feature that is located at a point of balance between Planck and CMB corresponding to two gamma rays  $1 \times 10^{-16}$  m and  $1 \times 10^{16}$  m. The matter antimatter annihilation process provides a lens to explore the Strong force relationship with the Gravitational force. Here the surface charge squared provides a gravitational lens, where the 38-orders of magnitude between the Strong force and Gravitational force are examined through the charge surface area parameter and the electric field distance between the layers of charges associated with the Charm quark (Weak force) and E/M fields of the opposite charges at  $n=1$  within the proton are given by 137 and the strength differences between the Strong force and the electromagnetic force.

$$(1.602 \times 10^{-19})^2 = 2.5664 \times 10^{-38} C^2 \quad (16)$$

The  $\Delta$ (space) and energetic force difference between the Strong force and the Gravitational force is associated with the surface areas of both charges and their attraction and distance between them. This proposed unification of the Strong force within the nucleus of the atom with the gravitational force corresponding to elementary charge squared provides the basis of unifying the opposite ends of the energy scales through this reciprocal inverted relationship.

The electromagnetic force at  $n=1$  in the electron (negative concave counterclockwise rotation) and positron (positive convex clockwise rotation) positioned at the  $n=1$  Lyman line electron transition layer of the Bohr model of the hydrogen atom corresponds to a barrier membrane thickness of 137. This relates to the strength of the force difference between the Strong Force (1) and the electromagnetic force

$$(1/137.174 = 0.00729). \quad (17)$$

This was modelled on the  $n=4$  electron transition at 1458 nm.

$$\frac{1458}{2} = 729 \times 1 \times 10^{-5} = 0.00729 \quad (18)$$

The connection with the strange quark electric field decay of its half-life  $1 \times 10^{-10}$  s. The 4th layer of the hydrogen s-orbital system provides a suitable model for the 16 parts of the He-BEC helium atom system. The modelling of the

wavelength 1458 nm for DE and DM modelling is outlined here.

$$\frac{1458}{12} = 121.6 \text{ nm And } \frac{121.6}{4} = 30.4 \text{ nm} \quad (19)$$

And

$$\frac{1458}{4} = 364.8 \text{ nm And } \frac{364.8}{12} = 30.4 \text{ nm} \quad (20)$$

The 12 and 4 features of 75% dark energy and 25% dark matter emitted from the He-BEC singularity through the alpha particle emission (12 out as DE) and (4 in as DM) at T0 are in alignment with the Brackett series  $n = 4$ , modelling the transition  $n = 4$  to  $n = 1$  of DE 12 at 121.6 nm and the transition  $n = 4$  to  $n = 2$  of DM 4 at 364.8 nm. Such transitions are proposed to be involved in a dynamic system operating in conjunction with other electron transitions to behave as the proton architect in the construction of atomic systems in biological regulation of pH, in a dynamic control exchanging protons between the DE and DM systems and the proton exchange between functional groups of biological molecules.

## 2.6 Proton quark connection to 30.4 nm

The proton is known to contain three quarks, UU and D. The Compton wavelength of U =  $5.6356 \times 10^{-13}$  m and D =  $2.5617 \times 10^{-13}$  m based on their rest masses.

$$U \times U \times D = 8.13596 \times 10^{-38} \text{ m}^3 \quad (21)$$

$$8.135 \times 10^{-38} / 6.67 \times 10^{-11} = 1.22 \times 10^{-27} \quad (22)$$

$$1 / 1.22 \times 10^{-27} = 8.20 \times 10^{26} \quad (23)$$

$$8.20 \times 10^{26} / c^3 = 30.4 \text{ nm}$$

This pathway unites the subatomic quark rest masses and the Strong Force with gravitational properties of the surface area elementary charge. There are 38-order of magnitude separating gravitational force strength from the Strong force.

$$(1.602 \times 10^{-19})^2 = 2.5664 \times 10^{-38} \quad (25)$$

$$8.13596 \times 10^{-38} \text{ m}^3 / 2.5664 \times 10^{-38} = 3.17 \quad (26)$$

This is connected to the proton's reciprocal half-life timing of

$$3.17 \times 10^{-43}$$

and the aromatic ring timing of

$$3.17 \times 10^{-19} \text{ nm/s}$$

The  $\Delta$  corresponding to

$$1 \times 10^{24}$$

that relates to the Charm quark's half-life timing of

$$1 / (1 \times 10^{-12})^2$$

## 2.7 Charm membrane separation of positive and negative surface charges

The following section on the Charm quark highlights its role

in the weak force within the proton in beta plus and beta minus processes, where the Weak force strength is  $1 \times 10^{-6}$  orders of magnitude smaller than the Strong force (1) and this corresponds to the Charm quark's electric field decay of its half-life  $(1 \times 10^{-12})^{0.5}$  s. The proton has recently been shown to contain a Charm quark for a brief time, and the He-BEC modelling of the Charm quark  $1.27 \times 10^9$  eV /c<sup>2</sup> provides several interesting relationships within the structure of the proton. This suggests that the Charm quark has a functional role to play in forming charge and mass in conjunction with the Higgs mechanism as outlined in the following section.

### 2.8 Charm quark rest mass modelled through the He-BEC approach

The He-BEC modelling routine is constrained by rules of charge conservation, where both positive and negative charges are formed simultaneously to maintain an overall zero-charge state. The initial charge state within the He-BEC singularity is also zero. This constraint places limitations on a system in which a positive charge is generated every time a negative charge is generated. Using an inverse square law reciprocal mathematical framework, a model was developed to unite opposite scales of atomic theory and cosmological composition. The initial wavelength in the He-BEC of

$$4 \times 10^{-14} \text{ m}$$

and its reciprocal

$$2.5 \times 10^{13} \text{ m}^{-1}$$

The multiplication of reciprocals gives 1, and the division of reciprocals gives r<sup>2</sup>.

The reciprocal features of the modelling approach align with an inverse-square law framework for quantum gravity. The relationship between kJ/mole (m/s) was used to establish cosmological (m/s) and (Pl/s) for the subatomic structure within the proton. This provides a direct inner-dimensional reflection of external reality from an internal subatomic process. The location of such a system in a biological molecule corresponds to the temporal features of the aromatic ring and its symmetry with the age of the universe, where the radius of the aromatic ring and the age of the universe demonstrate form and temporal function of a geometrically constrained spacetime. Here the radius of the aromatic ring corresponds to

$$1.39 \times 10^{-10} \text{ m}$$

and the age of the universe of

$$1.39 \times 10^{10} \text{ years}$$

This enables conversion between distance and time corresponding to the entire age of the universe rather than being limited by c and the emergence of c at 380,000 years. The aromatic ring time and distance conversion factors correspond to  $1 \times 10^{-20}$  m/year,  $1 \times 10^{-11}$  nm/year,  $3.17 \times 10^{-19}$  nm/s and  $3.17 \times 10^{-28}$  m/s. The aromatic ring temporal

toolbox acts as a lens to unlock the proton decay pathway, which previously has not been able to be identified. Here we can see the reciprocal half-life timing of the proton  $1 \times 10^{35}$  years or  $3.16 \times 10^{42}$  seconds corresponds to

$$3.17 \times 10^{-43} \text{ s}^{-1}$$

The relationship to the Top quark' half-life to the proton reciprocal half-life through the aromatic ring system is given by;

$$5 \times 10^{-25} \times 3.17 \times 10^{-19} = 1.59 \times 10^{-43} \text{ nm} \quad (27)$$

And

$$1.59 \times 10^{-43} \text{ nm} \times 2 = 3.17 \times 10^{-43} \text{ nm} \quad (28)$$

The Top quark's half-life of  $5 \times 10^{-25}$  is connected to the aromatic ring (nm/s) feature and provides the basis for the Up quark decay system hidden from view behind the Faraday cage of the aromatic ring. Modelling of the ring as a black hole singularity is also possible, with its event horizon giving an explanation for entropy.

$$S = (SA \times c^3)/(4 \times G \times \hbar) \quad (29)$$

$$S = 9.20 \times 10^{18} \quad (30)$$

Identification of the subatomic pathways within the proton in connection with the aromatic ring offers insight into a dynamic system unseen by measurement, due to its location and light processing speed, but able to be predicted and modelled biologically using proton tunnelling dynamics associated with pH and pKa of specific functional groups in molecules containing amine and carboxylic acids. The concentration of a substrate in mole/L functions as the reciprocal of kJ/mole in the He-BEC compression system of  $1/c^2$  in s/m and this provides a direct connection to the subatomic systems operating within the aromatic ring. The 14 orders of magnitude of pH 1-14 can then be explored biologically using the subatomic kJ/mole system in the He-BEC modelling of  $4E-14$  m as the initial wavelength and the 4 particles in the proton.

### 2.9 Modelling of the Charm quark rest mass

The Charm quark rest mass

$$1.27 \times 10^9 \text{ eV /c}^2 \quad (31)$$

corresponds to a Compton wavelength of

$$9.7625 \times 10^{-16} \text{ m} \quad (32)$$

and

$$1.23 \times 10^{11} \text{ kJ/mole (m/s)} \quad (33)$$

The hertz frequency is calculated using the following approach;

$$1/9.7625 \times 10^{-16} \text{ m} \times 1.23 \times 10^{11} \text{ m/s} = 1.26 \times 10^{26} \text{ s}^{-1} \quad (34)$$

And its reciprocal second timing for the Charm quark is given by

$$1/1.26 \times 10^{26} \text{ s}^{-1} = 7.97 \times 10^{-27} \text{ s} \quad (35)$$

This is similar to the He-BEC modelling of charge where

$$8 \times 10^{-27} \text{ m}^2 / 1.6 \times 10^{-35} \text{ m} = 5 \times 10^8 \quad (36)$$

And

$$4 \times 10^{-18} \text{ m} \times 2 \times 10^{-9} \text{ m} = 8 \times 10^{-27} \text{ m}^2 \quad (37)$$

This demonstrates that the electric field and magnetic field decay from the Planck system provides a point of interaction corresponding to the location and timing of the Charm quark. This corresponds to the location that unites mass and charge. It is the point of balance between the Planck system (DM) and the 1/h system (DE). Analysis outlined below also shows that this location is equivalent to 45.6 nm or 91.2 nm / 2. Modelling of the Charm quark based on its rest mass provides a way to explore the fluidic system that separates positive and negative surfaces in the formation of the electron and positron. Using the rearranged Einstein equation:

$$E/M = c^2 \quad (38)$$

corresponds to

$$4 \times 10^{-18} \text{ m} / 2 \times 10^{-9} \text{ m} = 2 \times 10^{-9} \quad (39)$$

and its reciprocal

$$1/2 \times 10^{-9} \text{ m} = 5 \times 10^8 \text{ m}^{-1} \quad (40)$$

and

$$M/E = 1/c^2 \quad (41)$$

$$2 \times 10^{-9} \text{ m} / 4 \times 10^{-18} \text{ m} = 5 \times 10^8 \quad (42)$$

This corresponds to the charge radius and surface area of the elementary charge determined using the following calculation;

$$(5 \times 10^8)^2 \times \pi \times 4 = 3.14 \times 10^{18} \text{ m}^{-2} \quad (43)$$

The reciprocal of the charge radius is given by

$$1/3.14 \times 10^{18} \text{ m}^{-2} = 3.18 \times 10^{-19} \text{ m}^2 \quad (44)$$

This corresponds to  $2 \times$  the elementary charge of the electron. One charged surface is concave and the other convex. The positive surface is convex and the negative concave. The rotation of the electron in the concave surface is counterclockwise, and the rotation (angular momentum) of the positron convex surface is clockwise. As both positive and negative surfaces are generated simultaneously, there is a conservation of charge constraint on the system that conserves the overall initial zero charge state. An individual surface corresponding to elementary charge is seen in the calculation given by:

$$3.18 \times 10^{-19} \text{ C} / 2 \approx 1.6 \times 10^{-19} \text{ C} \quad (45)$$

corresponding to the elementary charge of the electron.

Therefore, the  $\Delta(\text{space})$  is the surface area charge radius to

generate the elementary charge of the electron and positron through charge conservation (2e). One positive and one negative charge are generated simultaneously to maintain an overall zero-charge state. This identifies that charge conservation is fundamental to the model.

The relationship to the He-BEC model corresponds to

$$1 \times 10^{18} \text{ s} \times \pi = 3.14 \times 10^{18} \quad (46)$$

The half-life timing of the alpha particle emission from the He-BEC isotropic singularity corresponds to  $1 \times 10^{18}$  s and  $\pi$  is formed through the differential velocity between  $v$  and  $c$  as outlined below. The velocity  $v$  is determined by the initial  $\Delta$  He-BEC wavelength of  $4 \times 10^{-14}$  m, which corresponds to 2990700000 kJ/mole (m/s). What this demonstrates is that the initial state of the universe before the beginning of time predicts the process giving rise to the formation of elementary charge via the constraints of charge conservation. The initial state of the universe and its evolutionary development to generate the composition of the universe as we know today (67.74% dark energy, 27.42% dark matter, and 4.84% matter) can be modelled successfully when the correct initial state is identified.

The charge phenomena ( $\sigma e/S$ ), offering testable predictions for the attosecond-scale measurements ( $\sim 10^{-18}$  s). Such investigations could reveal whether charge emerges from the electron's spatial extension or boundary effects, potentially uncovering new electron characteristics beyond current quantum descriptions while addressing longstanding questions about charge quantization and distribution at fundamental scales.

Further calculations for the Charm quark rest mass of

$$1.27 \times 10^{-9} \text{ eV/c}^2 \quad (47)$$

corresponds to

$$7.97 \times 10^{-27} \text{ s}' \text{ and } 125 \text{ s}''$$

$$7.97 \times 10^{-27} \text{ s}' \times 125 \text{ s}'' = 1 \times 10^{-24} \text{ s}^2 \quad (48)$$

$$\sqrt{1 \times 10^{-24}} \text{ s}^2 = 1 \times 10^{-12} \text{ s} \quad (49)$$

That corresponds to the half-life timing of the Charm quark. The SUSY inversion models calculations of temporal locations of time-space. The first Charm quark timing is aligned to the nodal position of  $(h)E^{0.5} \times (h)M^{0.25}$ . The second timing of 125 s linked to the Higgs Boson mechanism and its rest mass of  $125.11 \times 10^9 \text{ eV/c}^2$ . The  $1 \times 10^{-9}$  s is associated with a molecule decay of the hydroxyl radical, which is aligned with the alpha particle half-life timing of the He-BEC through inverse square law where

$$1 \times 10^{18} \text{ s} = 1 / (1 \times 10^{-9})^2 \text{ s} \quad (50)$$

The hydroxyl radical's half-life timing and its role in biological systems provides an inverse square law timed memory system. The conversion of the aromatic ring temporal storage of time energy into energy used for healing and regeneration requires the hydroxyl radical's energy to

break open the aromatic ring. The release of energy from the ring occurs in such a way, as to provide time energy for the body to restore well-being.

### 2.10 Muon and Tau half-life timings and four times elementary charge

The elementary charge in the positron and electron systems is seen through the subatomic particle half-life timings of the muon and tau particle.

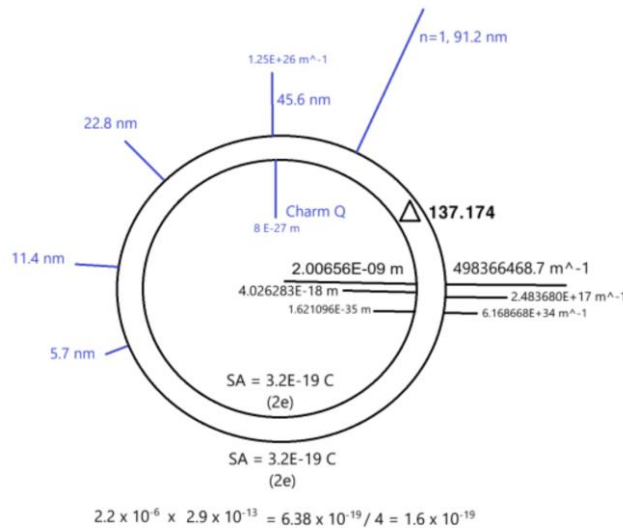


**Fig. 1:** Four times elementary charge photonic bubble model at n=1 having a 137-bubble membrane thickness preventing matter antimatter annihilation

The half-life of the Muon  $2.2 \times 10^{-6}$  s and Tau particle at  $2.9 \times 10^{-13}$  s where

$$2.2 \times 10^{-6} \times 2.9 \times 10^{-13} = 6.38 \times 10^{-19} \text{ s}^2 \quad (51)$$

$$6.38 \times 10^{-19} \text{ s}^2 / 4 = 1.6 \times 10^{-19} \text{ C} \quad (52)$$

And this is equivalent to 4× elementary charge. Considering

$$4 \pi 1 \times 10^{-7} = \mu_0 \quad (53)$$

The timing of half-life related to  $\pi$  generation through differential velocity, was identified through the analysis of differential velocity where the DM inward compression velocity goes from  $\sqrt{v}$  to  $\sqrt{c}$ . This decrease in velocity does work in the system to create the  $\pi$  system. As it is also undergoing expansion within the DM system going from  $4 \times 10^{-14}$  m to  $1 \times 10^{-7}$  m through the transition corresponding to  $\sqrt{4} \times 10^{-14}/2$ . The vacuum is therefore involved in the generation of  $\pi$  particle systems based on the differential velocities identified through the modelling of v and c.

$$\frac{(\sqrt{v} + \frac{1}{\alpha})}{(\sqrt{c} + \frac{1}{\alpha})} = \pi \quad (54)$$

where  $\alpha$  is the fine structure constant, which can be obtained via several processes leading to the calculation given by the following pathways. The 1458 nm wavelength n=4 hydrogen electron transition having already been mentioned as a DE and DM modelling system. As the aromatic ring

contains carbon atoms that contain 6 protons with 3 quarks and a total of 12 quarks in a 3:1 ratio DE : DM giving 9:3, the interaction of wavelengths to the 720 rotation of the aromatic ring bring into the containment facility where the dynamic interplay between the internal environment with the Faraday cage nature of the ring and its makeup of atomic systems gives rise to a convergence on the number 729. As there are 27-orders of magnitude in cosmic inflation as well as 27 orders in proton tunnelling to the n=1 position of the electron in the Bohr model.

$$729 = 9^3 \text{ or } 3^6 \text{ or } (1458 / 2) \text{ or } 27^2 \quad (55)$$

And

$$1/(729 \times 1 \times 10^{-5} = 0.00729) = 137.1742112 \quad (56)$$

The electric field decay of the Strange quark is proposed to be involved.

$$(1 \times 10^{-10})^{0.5} \quad (57)$$

The initial He-BEC singularity wavelength also determined the ionization energy of the electron at the n=1 position in the proton.

$$\frac{\sqrt{v^3 \times c^3}}{1 \times 10^{-9} \times \frac{1 \times 10^{35}}{1.6}} = 13.58 \quad (58)$$

This shows the prediction of electron ionization in hydrogen at n=1, 91.2 nm and 1311.7 kJ/mole, and 13.58 eV. The number, 13.58 is observed for the bottom-quark second derivative of its timing, 13.58 s" in the analysis performed for the rest mass of the Bottom quark based on  $4.18 \times 10^9$  eV/c<sup>2</sup>. This corresponds to  $2.9661 \times 10^{-16}$  m,  $1.0107 \times 10^{24}$  Hz and  $4.0331 \times 10^{11}$  kJ/mole. The s" timing feature of the Bottom quark is obtained using the kJ/mole inverted meter ( $3.37 \times 10^{15}$  m<sup>-1</sup>) and the reciprocal calculation;

$$3.37 \times 10^{15} \times 4.0331 \times 10^{11} = 1.36 \times 10^{27} \text{ s}^{-1} \quad (59)$$

and second timing of  $7.35 \times 10^{-28}$  s. The half-life of the Bottom quark corresponding to  $1 \times 10^{-13}$  s × the kJ/mole velocity for the Bottom quark corresponds to  $4.03 \times 10^{-2}$  m" the second-meter position. This location is used to calculate the kJ/mole velocity for the second-meter wavelength position ( $2.97 \times 10^{-3}$  kJ/mole). The reciprocal second-meter position is then calculated ( $24.8 \text{ m}^{-1}$ ), followed by the Hz frequency ( $7.44 \times 10^9$  Hz) and then the reciprocal second timing ( $7.36 \times 10^{-2} \text{ s}^{-1}$ ) for this location, which provides the timing for this location to correspond to (13.587 s). The two timings for the Bottom quark correspond to  $7.35 \times 10^{-28}$  s" and 13.586 s"

where

$$7.35 \times 10^{-28} \text{ s}'' \times 13.586 \text{ s}''' = 9.99 \times 10^{-27} \text{ s}^2 \quad (60)$$

and

$$\sqrt{9.99 \times 10^{-27}} = 1 \times 10^{-13} \text{ s} \quad (61)$$

and this corresponds to the half-life for the Bottom quark. Rather than just seeing the half-life timing as a decay parameter, the modelling provides an approach to explore time as a reciprocal system in the rest mass of the particle

own inertial reference frame and this is aligned with Einstein's thinking regarding space telling matter how to move and matter tells space how to curve. The kJ/mole velocity corresponds to the motion of space, where its relative velocity to  $c$  will induce a compression of space if  $\text{kJ/mole} < c$  and expansion of space when  $\text{kJ/mole} > c$ . Modelling of subatomic particles velocity based on their kJ/mole (m/s) velocity therefore alters the expansion and compression of space itself. The conservation of velocity also occurs in this model. Here the outward  $v$  is conserved by an inward  $\nabla v$  velocity. This approach maintains conservation of energy under specific conditions of geometric form and ratio. Analysis of both particle formation through differential velocities as well as compression and expansion of space based on binding energy and half-life timings corresponding to the rest mass provides a relativity based subatomic analysis where  $\log(\text{kJ/mole})$  vs  $\log(\text{nm})$  provides a quantum gravity framework based on inverse square law.

### 2.11 He-BEC and the 1 second radius of the condensate and the Bottom quark rest mass

$V$  is determined to be 2990700000 kJ/mole based on  $\Delta 4 \times 10^{-14}$  m in the ground state wavelength of the He-BEC isotropic singularity. The initial state of the universe with an inertial rest frame of  $r = c$  as the solution for the radius of a black hole singularity based on the Schwarzschild radius of a black hole solution to Einstein's equations. As the radius is also equivalent to the distance light travels in a vacuum in 1 second, then the radius and inertial frame of reference for the singularity is equivalent to 1 second, and  $r = 1$  s. Therefore, both time and distance have an inertial framework corresponding to  $c$  at 299792458 m/s. It is interesting to note that the Bottom quark has a rest mass like a 1 second volume of  $4.18879 \text{ s}^3$ . The link to the ionization energy of the electron and the 1 s volume rest mass provides an interesting lens through which to explore temporal processes within subatomic pathways operating within the proton. Such pathways have been unable to be observed using high-energy collisions in colliders but are becoming increasingly evident during the modelling of proton tunnelling in biological systems, when the aromatic ring acts as the lens through which to observe functional processes hidden from measurement.

#### 2.11.1 Biological Implication

The electron's quantum mechanical description through wave functions characterizes its position, velocity, and angular momentum, yet this probabilistic framework provides limited mechanistic insight into its biological operation. Crucially, electrons drive biological energy transduction, particularly in mitochondrial electron transport chains, where they enable ATP synthesis by establishing proton gradients. This requires hydrogen atom ionization with 13.58 eV energy input to separate electrons from protons, yielding charged species essential for bioenergetics. The relationship between  $13.58 \text{ nm} = 91.2 \text{ eV}$  and  $91.2 \text{ nm} = 13.58 \text{ eV}$  provides a reciprocal relationship

between energy and distance. As shown above, the eV of 13.58 is derived from the differential velocity from the He-BEC model based on first-principle calculations as well as linked to the Bottom quark  $s''$  featured temporal location.

The proton's internal structure as a quark-gluon plasma - comprising three quarks (two Up and one Down) bound by gluons - exhibits both electromagnetic charge sensitivity and pH-dependent behaviour. Remarkably, aqueous phase proton concentrations can model quark-gluon plasma dynamics without extreme temperatures, suggesting parallels to pre-atomic universe conditions. The electron-proton binding via Coulomb attraction ( $F = k(e^2/r^2)$  where  $e = 1.602 \times 10^{-19} \text{ C}$ ) creates electrically neutral systems despite the fundamental distinction between QCD colour charge and electromagnetic charge. From a biological perspective, the electron's charge may emerge from geometric properties, with surface area calculations ( $3.14 \times 10^{18} \text{ s}$  for a spherical bubble model with radius  $2.00656 \times 10^{-9} \text{ m}$ ) closely approximating the elementary charge ( $3.2 \times 10^{-19} \text{ J} = 2e$  through charge conservation principles). This model, derived from an electron diameter of  $4.026 \times 10^{-18} \text{ m}$ , intriguingly connects to Planck-scale dimensions ( $1.62108 \times 10^{-35} \text{ m}$  via diameter squaring). Biologically, electrons mediate both molecular bonding and elemental periodicity through their shared occupancy with protons, while their mitochondrial flux through complexes I-IV drives oxidative phosphorylation. The quark-level proton structure (uud) versus neutron (udd) composition, with mass differences ( $mu \approx 2.2 \text{ MeV/c}^2$ ,  $md \approx 4.84 \text{ MeV/c}^2$ ), maintains distinct nuclear identities despite charge neutralization when bound to electrons. This unified framework spans quantum mechanics, particle physics, and biochemistry, revealing how fundamental charge properties manifest across biological organization levels from subatomic quarks to metabolic pathways.

The link between vacuum of space at Planck  $1.6 \times 10^{-35} \text{ m}$  and  $n = 1$  position of the electron at  $5.7 \times 10^{27}$  Planck lengths is associated with charge generation through tunnelling, where cosmic inflation and the proton tunnelling processes are aligned through a ratio of 1 m : 1 Planck length. The velocity of space at Planck corresponds to  $7.4767 \times 10^{30} \text{ kJ/mol}$ , and

$$7.4767 \times 10^{30} / 5.7 \times 10^{27} = 1311.7 \text{ kJ/mol} \quad (62)$$

or the angular momentum at  $n = 1$  is  $91.2 \text{ nm}$  and  $13.58 \text{ eV}$ .

The biological significance of the electron is seen in the mitochondrial electron transport chain (ETC) and the generation of energy within cells in the form of ATP. The electron is involved in bonding in molecules and between molecules, where bonds are the sharing of electrons. It is proposed that there is one electron per proton in an atom, and this allows classification of the elements of the periodic table.

The bond length of  $0.139 \text{ nm}$  is nearly 3 orders of magnitude smaller than the  $n = 1$  location of the electron in hydrogen

at 91.2 nm. This suggests that the sharing of electrons may not be the actual process responsible for bonding between atoms. A more appropriate interpretation may be that the electron can tunnel into the neighbouring atom's nucleus, allowing it to become a quark. This provides an energy conservation exchange with the atom quark being emitted out of the nucleus to become the required orbital particle. Such interactions would align with the features of beta-plus and beta-minus decay in the SUSY inversion modelling of isotope decay physics. If one considers the ability of the universe to create bonds in molecules and its ease in creating living dynamic systems that operate in coherent states, our Newtonian modelling of atomic structure in biological systems is a far cry from the elegance that operates within ourselves through the temporal dynamic subatomic pathways. Biomimicry attempts to use natures approaches to do things. Learning the rules of nature at a quantum level has been challenging due to the counter intuitive nature of the inversion reciprocal system. The He-BEC model offers a solution to the missing antimatter in cosmology and provides an exploratory pathway to investigate subatomic systems through the laws of conservation. The conservation of charge is explored in the following section.

### 3 Quark Charge Calculations

There are a potential number of approaches that can be used to determine a quark charge giving the proton with an overall charge of +1 and a neutron with a charge of 0. Various research papers have been published involving quark charge and their application to different systems as well as large experiments at particle colliders like the LHC, look at the following references [9-41]. The standard approach is to use fractions and add those together so that Up quarks have a fractional charge of  $+\frac{2}{3}$  and the Down quark has a fractional charge of  $-\frac{1}{3}$ .

The proton is made up of two Up quarks and one Down quark, and the neutron is made up of one Up quark and two Down quarks. The standard model uses fractional charges for the quarks, up  $+\frac{2}{3}$  and down  $-\frac{1}{3}$  and adds these charges together to get the total charge for the proton and neutron. For the proton's charge, the standard model calculation is:

$$+\frac{2}{3} + \frac{2}{3} - \frac{1}{3} = +1 \quad (63)$$

For the neutron's charge, the standard model calculation is:

$$+\frac{2}{3} - \frac{1}{3} - \frac{1}{3} = 0 \quad (64)$$

In our model, it is proposed to utilize whole numbers rather than fractions and multiply the quark charges together rather than summing them. By revising the quark charge calculations for protons and neutrons using whole numbers instead of fractions and using multiplication instead of addition, the proton charge remains positively charged, however, the neutron charge becomes negative, requiring a positron to be added to maintain the observed zero charge for the neutron within the nucleus of the atom. The standard quark charge calculations and an alternative methodology

are provided in Figure 2.

Thus, we can see that the Up quark in the SUSY inversion quark charge calculation framework has a -1 charge and the Down quark +1.

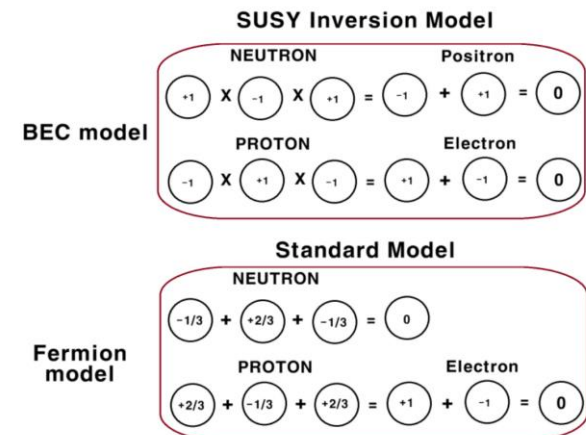


**Fig. 2:** Quark charge calculations for BEC model (bosons) and Standard Model (fermions)

The SUSY inversion model proposes that the Up quark has a charge of -1 and the Down quark has a charge of +1, and instead of adding the charges, the charges are multiplied together to get the total charge for the proton (+1) and neutron (-1).

For the proton, the SUSY inversion calculation is:

$$(-1) \times (+1) \times (-1) = +1 \quad (65)$$

For the neutron, the SUSY inversion calculation is:

$$(+1) \times (-1) \times (+1) = -1 \quad (66)$$

This revised charge model proposes that while protons maintain their characteristic positive charge, neutrons acquire a net negative charge that requires compensation by an embedded positron to achieve the observed neutral state (0). The framework suggests the presence of antimatter (positrons) within atomic structure, particularly localized in the superfluid Bose-Einstein condensate (BEC) phase of helium-4 at cryogenic temperatures ( $T \sim 2.17$  K near absolute zero). This configuration preserves charge neutrality while introducing antimatter as an essential structural component of stable nuclei.

The proton charge is calculated using multiplication:

$$-1 \times +1 \times -1 = +1 \quad (67)$$

and the neutron:

$$+1 \times -1 \times +1 = -1 \quad (68)$$

Within the SUSY inversion framework, the neutron carries a net charge of -1, contrasting with the Standard Model's prediction of neutrality. To reconcile this discrepancy while preserving charge conservation, the model introduces a positron ( $e^+$ ) as an intrinsic structural component of the neutron. This antimatter counterpart exactly cancels the



formation of atoms. Such pathways are evident in the model of the proton developed using the subatomic particles in conjunction with the quantum lens of the aromatic ring  $3.17 \times 10^{-19}$  nm/s.

### 3.2 Charge Cancellation in the Neutron

We model the neutron as a composite state of a three-quark core with multiplicative charge  $-1$  and an embedded positron of charge  $+1$ :

$$|n\rangle = |n_{\text{core}}\rangle \otimes |e+\rangle, \quad (77)$$

Where

$$Q_{\text{core}} = \prod_{i=1}^3 Q_{q_i}^{\text{rev}} = (-1) \times (+1) \times (+1) = -1,$$

$$Qe^+ = +1 \quad (78)$$

Introduce the total charge operator

$$Q^{\wedge} = Q^{\wedge}_{\text{core}} + Q^{\wedge}_{e^+}. \quad (79)$$

By definition of its action on each substrate,

$$Q^{\wedge}_{\text{core}}|n_{\text{core}}\rangle = -1|n_{\text{core}}\rangle, Q^{\wedge}e^+|e+\rangle = +1|e+\rangle \quad (80)$$

Hence on the full neutron state:

$$Q^{\wedge}|n\rangle = (Q^{\wedge}_{\text{core}} + Q^{\wedge}_{e^+})|n_{\text{core}}\rangle \otimes |e+\rangle = (-1 + 1)|n_{\text{core}}\rangle \otimes |e+\rangle = 0|n\rangle \quad (81)$$

Therefore, the negatively charged three-quark core is exactly balanced by the embedded positron, rendering the neutron electrically neutral.

## 4 Consequences of the Revision of Quark Charge Calculations

The SUSY inversion framework revolutionizes atomic structure by fundamentally revising quark charge assignments, revealing that the neutron possesses an intrinsic negative charge ( $Q_n = -1$ ) requiring compensation by an embedded positron ( $e^+$ ) to achieve the observed neutrality. This establishes perfect baryonic symmetry through complementary matter-antimatter pairs: proton-electron ( $p+e^-$ ) and neutron-positron ( $n-e^+$ ), resolving both the atomic charge neutrality condition and the cosmological matter-antimatter asymmetry problem. The presence of positrons, first detected by Anderson in 1932, suggests that the “missing” antimatter may reside within the atomic structure all along and be observed through charge conservation calculations on the outer leaflet of the convex surface of the spherical electron, negatively charged inner leaflet. Applied to the helium-4 atom, this model predicts 16 fundamental particles: 12 quarks (6 up, 6 down) comprising two protons ( $2 \times uud$ ) and two neutrons ( $2 \times udd$ ), plus two orbital electrons and two orbital positrons. This configuration maintains exact charge balance

$$\Sigma Q = [6 \times (+1) + 6 \times (-1)]e^+ + [2 \times (-1) + 2 \times (+1)]e^- = 0 \quad (82)$$

while achieving matter-antimatter parity, with experimental signatures potentially detectable in superfluid helium-4

Bose-Einstein condensates, neutron star matter, and high-energy collision experiments.

The He-BEC isotropic singularity state identifies the ground wavelength of  $4 \times 10^{-14}$  m and its reciprocal of  $2.5 \times 10^{13}$  m $^{-1}$ . The multiplication of these provides 1 and the division gives  $1.6 \times 10^{-27}$  m $^2$ . The  $\Delta$  to Planck  $1.6 \times 10^{-35}$  m is  $1 \times 10^8$  and

$$\sqrt{1 \times 10^8} = 1 \times 10^4 \quad (83)$$

giving

$$1 \times 10^8 / 1 \times 10^4 = 1 \times 10^4 \quad (84)$$

and

$$4 \times 10^{-14} \times 1 \times 10^{-4} = 4 \times 10^{-18} \quad (85)$$

corresponding to the Planck

$$(1.6 \times 10^{-35})^{0.5} = 4 \times 10^{-18} \text{ m} \quad (86)$$

This subatomic temporal and spatial location appear to be a point of balance that maintains the conservation of energy. It appears to be a process linked to the Charm s' timing at  $8 \times 10^{-27}$  m $^2$  (s'), where

$$8 / 1.6 = 5 \quad (87)$$

There appears to be a 5 second rule corresponding to the surface area of 5 seconds that corresponds to  $100 \pi$  (314.1592654). The differential velocity provides a tool to see  $\pi$  formation from the He-BEC modelling. There also appears to be an important timing associated with 3 seconds. This timing corresponds to a point of balance between the surface area to volume ratio linked to  $113.0973 / 113.0973 = 1$ . This is proposed to be associated with particle formation linking the  $3r^{-1}$  features of quarks to the orbital particle in the proton + electron and neutron + positron. The positron and electron interaction through annihilation to generate two gamma ray photons of equal energy provides a system to illuminate the subatomic structure within the atom. The various competing subatomic pathways provide useful exploratory tools to reveal contrasting systems operating beyond the limitation of measurement.

### 4.1 Emergence of light within cosmology and the temporal boundary within atomic structure

Atoms contain an electromagnetic field. The emission and absorbance of photons by atoms is associated with the motion of the electron in the orbital layers of the atom. The gluons contain photons within the colour charge of the atom. The proton modelling provided evidence from the n=4 Brackett line electron transition that corresponds to 16 parts at 1458 nm and this halved gives 729. As outlined above, 729 is associated with the Charm quarks role as a magnetic barrier separating positron and electron outer-leaf charge radii and inner-leaf charge radii within modelling of charge formation tunnelling system. This wavelength analysed using the DE and DM modelling approach generated  $48 \times 30.4$  and this linked to UDU proton quark wavelengths through this analysis methodology. Here,  $30.4 \text{ nm} \times 3 = 91.2$  nm and the location of the electron in n=1 of the hydrogen atom. Our charge analysis approach using the He-BEC

isotropic singularity gives rise to a surface area to volume system linking (Vol / SA) / radius = 3. Other attributes of the hydrogen atom orbital modelling offer insight to the transitions and differential velocities of the wavelengths generated through the relative motion of the positron and electron pairings (this will be presented elsewhere). The n=3 alignment with the aromatic ring Higgs mechanism have been identified and will be presented in a separate paper.

#### 4.2 The Embedded Positron Hypothesis and $\beta$ -Decay Processes

The origin of positrons in  $\beta$ -decay presents intriguing questions about mass asymmetry and stability differences between nucleons. The neutron's greater mass ( $m_n = 939.565 \text{ MeV}/c^2$  vs  $m_p = 938.272 \text{ MeV}/c^2$ ) despite both being three-quark hadrons, along with the neutron's instability via  $\beta^-$  decay ( $n \rightarrow p + e^- + \bar{\nu}_e$ ) compared to the proton's extreme stability ( $\tau_p \sim 1 \times 10^{35} \text{ s}$ ), reveals fundamental asymmetries in nuclear structure. The SUSY inversion model explains these observations by proposing that the neutron contains an embedded positron, accounting for both its additional mass ( $\Delta m \approx m_{e+} = 0.511 \text{ MeV}/c^2$ ) and its decay mechanism through positron emission. Conversely, while the proton-electron system also achieves charge neutrality, the proton itself remains stable against  $\beta^+$  decay in free space due to energy conservation constraints and the balance of  $uu = d$  and  $- - = +$ . Here,  $2.2 \times 2.2 = 4.84$  and  $\sqrt{4.84} = 2.2$ , highlighting the internal balance of energy providing the basis of stability. The d (888 s) half-life generating uu provides a timed duplication system and the addition of charges for the three quarks in the free proton gives -1 that offsets the +1-proton charge providing multiple charge states and a zero balanced state for the free proton if one considers these -1 charges within the nucleus associated with the Up quark. The mass of the electron is obtained through the following process:

$$d = 888 \times \text{Muon } 2.2 \times 10^{-6} \text{ s} = 0.0019536 \text{ s}^2 \quad (88)$$

$$1/0.0019536 = 511.875511876 \text{ s}^{-2} \times 1 \times 10^3 \quad (89)$$

$$= 5.11 \times 10^5 \text{ s}^{-3} \text{ eV} / c^2 \quad (90)$$

This reciprocal second volume was created through the interactions of the Muon's half-life, the Down quark's half-life, and the magnetic field decay of the Charm quark's half-life. The relationship between the Muon's half-life ( $2.2 \times 10^{-6} \text{ s}$ ) and the Up-quark's rest mass of  $2.2 \times 10^6 \text{ eV}/c^2$  is seen:

$$2.2 \times 10^{-6} \times 2.2 \times 10^6 = 4.84 \quad (91)$$

Where the Charm quark's electric fields decay corresponding to

$$1/1 \times 10^{-6} = 1 \times 10^6 \text{ s}^{-1} \quad (92)$$

is involved in giving

$$4.84 \times 10^6 \text{ eV} / c^2$$

providing a process for the generation of the Down quark. The  $\beta^-$  decay energy conservation rules correspond to the Down quark  $d+ \leftrightarrow e^-$  through tunnelling and charge

inversion as the quark exits within the nucleus of the atom. The positron  $p^+$  tunnels into the nucleus to become the new Up quark  $u^-$  and a newly formed proton is generated  $p^+ \leftrightarrow u^-$ . The rearrangement of charge and energy conservation process provides the basis for the connection of  $e^+ 75 \text{ s}$  with  $5625 \text{ s}^2$  where

$$625 = 1/1.6 \times 1 \times 10^2 \text{ s} \quad (93)$$

Strange quark system

$$\text{Strange } M^{0.25} 1 \times 10^{-8} \text{ s} \quad (94)$$

As shown above  $5 = 8/1.6$  and  $1 \times 10^3$  are associated with the magnetic field of the Charm  $1 \times 10^{-12} \text{ s}$ ,  $0.25 = 1 \times 10^{-3} \text{ s}$  and its reciprocal  $1 \times 10^3$ . The cosmic microwave background wavelength of  $1.6 \times 10^{-3} \text{ m}$  is associated with  $1 \times 10^3$  and the formation of 1.6 linked to the 8 parts being formed within the GR framing of  $8\pi$ .

This links to Charm s' timing at  $8 \times 10^{-27} \text{ m}^2$  (s') and  $1 \times 10^{18} \text{ s}$  alpha particle emission timing of the He-BEC isotropic singularity where

$$1 \times 10^{18} \text{ s} \times 1 \times 10^9 \text{ s} = 1 \times 10^{27} \text{ s}^2 \quad (95)$$

$$8 \times 10^{-27} \text{ m}^2 \times 1 \times 10^{27} \text{ s}^2 = 8 \text{ m}^2 \text{ s}^2 \quad (96)$$

These temporal and spatial calculations provide a framework in which to explore subatomic processes below the limits of measurements. The  $8\pi$  of GR and the unique loci of the aromatic ring within which the subatomic particles operate enables integration and unification of multiple physics models within the geometry and functionality of the aromatic ring and its associated spatial temporal multidimensional channel. This appears to be a fundamentally important loci that has biological implications for consciousness research along with having attributes of time linking structure to temporal function associated with memory formation and recall.

Nuclear processes exhibit distinct  $\beta$ -decay pathways:

$\beta^-$  decay:  $n \rightarrow p + e^- + \bar{\nu}_e$  (free neutron,  $\tau_{1/2} \approx 888 \text{ s}$ ) (97)

$\beta^+$  decay:  $p \rightarrow n + e^+ + \nu_e$  (bound proton in nuclei only)

The identification of the involvement of the aromatic ring in the  $UU = D$  system and  $DD = \text{?}$  precession angular momentum provides a process rather than a stable framework of particles that is present in a biological system. To a quantum biologist, this provides a system of subatomic pathways operating within living systems and not the stable atom veneer obtained through the use of proton, neutron and electron Newtonian space-filler protein structural models. Seeing what is potentially going on beneath the surface of atomic stability is demonstrating how dynamic and complex quantum biology appears to be when subatomic systems can be modelled using conservation rules. This provides a more deterministic feel that a biologist is used to compared to the probability and wavefunction collapse currently used in atomic theory based on quantum mechanics.

The  $1 \times 10^{32}$  fold difference in nucleon lifetimes provides compelling evidence for the neutron's composite structure n

$\equiv$  (udd)core +  $e^+$  (hidden positron model), where the incorporated positron resolves three key phenomena: (1) the mass difference  $\Delta m_{n-p} \approx 1.293$  MeV/c<sup>2</sup>, (2) the  $\beta^-$  decay pathway via positron emission, and (3) charge balance maintenance in stable nuclei. This framework suggests the apparent matter-antimatter asymmetry may reflect spatial separation rather than fundamental imbalance, with antimatter (positrons) localized within nuclei while matter (electrons) occupies atomic orbitals. The temporal separation of the positron and electron is observed, where the half-life timing of 1 s for the electron and 75 s for the positron are proposed. The electron at  $n=1$ , 91.2 nm obtained from the calculations outlined in subsection 2.6. The neutron calculations (DDU) correspond to:

$$\begin{aligned}
 (2.5617 \times 10^{-13})^2 \times 5.6356 \times 10^{-13} &= 3.7 \times 10^{-38} \text{ m}^3 \\
 3.7 \times 10^{-38} \text{ m}^3 / G &= 5.54 \times 10^{-28} \text{ s}^2 \text{ kg} \\
 1 / 5.54 \times 10^{-28} \text{ s}^2 \text{ kg} &= 1.8 \times 10^{27} \text{ s}^{-2} \text{ kg}^{-1} \\
 1.8 \times 10^{27} \text{ s}^{-2} \text{ kg}^{-1} / c^3 &= 66.94 \text{ nm} \\
 66.94 \text{ nm} \times 3 &= 200.81 \text{ nm}
 \end{aligned} \tag{98}$$

Comparing the protons quark system locating the electron at  $30.4 \times 3 = 91.2$  nm, the neutron's quarks system places the positron at  $66.94 \text{ nm} \times 3 = 200.81$  nm. The electron and positron are therefore both spatially and temporally separated preventing annihilation. At each location within the atom within these locations the electrons angular momentum velocity is 1311.7 kJ/mole and that for the positron is 595.72 kJ/mole. The differential velocities and timings based on the half-life values provides a toolbox to model their functional properties with respect to various potential pathways that operate within the subatomic systems of the proton. Annihilation is one such pathway that contributes to the generation approximately 0.1% of photons present in the universe.

Alternatively, the modelling suggests that the positron resides on the outside surface of the magnetic barrier arising from the  $1/h = 6.25 \times 10^{34} \text{ m}^{-1}$  SUSY inversion model. It is proposed to be linked to the positron half-life timing of 75 s via the cosmic microwave background (CMB). The elementary charge of  $1.602 \times 10^{-19} \text{ C}$  links to the CMB at  $1.6 \times 10^{-3} \text{ m}$  and Planck distance  $1.6 \times 10^{-35} \text{ m}$  via a  $\Delta 1 \times 10^{-16}$  and  $\Delta 1 \times 10^{16}$  giving  $\Delta 1 \times 10^{32}$  between CMB and Planck. This positional process is linked to E and B fields of the Planck vacuum for elementary charge formation via the Charm quark's positioning within the tunnelling process at  $8 \times 10^{-27} \text{ s}'$  and  $125 \text{ s}''$ . This modelling aligns each atom with a cosmological fractal and a single atom framework. It provides a location of spacetime within the atom by modelling the subatomic particles based on rest mass  $s'$ ,  $m'$ ,  $s''$ , and  $m''$ . Such a configuration enables novel interpretations of nuclear architecture and provides an approach to unify matter-antimatter symmetry through position-dependent manifestation and provides an alternative approach to quark charge calculations. Remarkably, the geometric foundations shared by Newtonian gravity and General Relativity offer a natural mathematical bridge for exploring these phenomena,

potentially reconciling quantum and classical descriptions of nuclear processes through their common underlying geometric structure within the confines of the aromatic ring.

#### 4.3 Positron Bound in a Neutron as a Spherical Potential Well

Let us consider a model of a positron bound in a neutron as a spherical potential well. Assuming the neutron provides a spherically symmetric potential well of radius  $R_n$  and depth  $V_0 > 0$ . The potential is defined as:

$$\text{For } 0 \leq r < R_n: V(r) = -V_0 \tag{99}$$

$$\text{For } r \geq R_n: V(r) = 0. \tag{100}$$

We look for a bound positron state ( $E < 0$ ) satisfying the time-independent Schrodinger equation:

$$-\hbar^2 / 2m_e \nabla^2 \psi + V(r)\psi = E\psi \tag{101}$$

where  $m_e$  is the positron mass. For an s-wave ( $l = 0$ ), we set  $\psi(r) = u(r)/r$ . The radial equation becomes:

$$-\hbar^2 / 2m_e d^2 u / dr^2 + V(r)u = Eu \tag{102}$$

Inside the well ( $r < R_n$ )

$$\text{Define: } k^2 \equiv 2m_e(V_0 + |E|) / \hbar^2 \tag{103}$$

$$\text{The equation simplifies to: } d^2 u / dr^2 + k^2 u = 0. \tag{104}$$

$$\text{The solution is: } u(r) = A \sin(kr) \tag{105}$$

Outside the well ( $r \geq R_n$ )

$$\text{Define: } \kappa^2 \equiv 2m_e|E| / \hbar^2 \tag{106}$$

The equation becomes:

$$d^2 u / dr^2 - \kappa^2 u = 0 \tag{107}$$

The normalized solution is:

$$u(r) = B e^{-\kappa r} \tag{108}$$

Matching at  $r = R_n$

Continuity of  $u$  and  $u'$  gives:

$$A \sin(kR_n) = B e^{-\kappa R_n} \tag{109}$$

$$A k \cos(kR_n) = -B \kappa e^{-\kappa R_n} \tag{110}$$

Eliminating A/B yields the quantization condition:

$$k \cot(kR_n) = -\kappa \tag{111}$$

Existence of at least one bound state

$$\text{Let: } \eta \equiv kR_n, \xi \equiv \kappa R_n, \tag{112}$$

$$\text{so: } \eta^2 + \xi^2 = 2m_e V_0 R_n^2 / \hbar^2 \equiv \rho^2 \tag{113}$$

Equation (1) becomes:

$$\eta \cot \eta = -\sqrt{\rho^2 - \eta^2} \tag{113}$$

The smallest nontrivial root  $\eta$  lies in  $(\pi/2, \pi)$ . A

bound state exists if and only if:

$$\rho > \pi/2, \text{ i.e., } V_0 > \hbar^2 \pi^2 / 8m_e R_n^2 \tag{114}$$

Using  $m_e c^2 \simeq 0.511$  MeV,  $\hbar c \simeq 197$  MeV fm, and  $R_n \sim 1$  fm, we estimate:

$$\frac{\hbar^2 \pi^2}{8m_e R_n^2} \sim \frac{(197 \text{ MeV} \cdot \text{fm})^2 \pi^2}{8(0.511 \text{ MeV})(1 \text{ fm})^2} \approx 20 \text{ MeV} \quad (115)$$

Thus, if the neutron well depth  $V_0 \geq 20$  MeV, there will be at least one s-wave bound state. As  $D \times D = 23.5 \times 1 \times 10^{12}$  and the Charm quarks electric field decay corresponding to  $1 \times 10^{-6}$  s provides a counterbalance to the additional  $1 \times 10^6$ , then we have identified the well in which the positron resides through the earth's precession calculation. The positron and neutron decaying timings offering the reason for the precession timings for Earth's seasons.

Under modest assumptions ( $R_n \approx 1$  fm,  $V_0 \geq 20$  MeV), the quantization condition (1) admits a solution  $E < 0$ , meaning a positron can be trapped in the neutron's potential well. The binding energy  $|E|$  is found by solving:

$$k \cot(kR_n) = -\sqrt{2m_e|E|/\hbar^2} \quad (116)$$

#### 4.3 Deep Inelastic Scattering in the Parton Model

We consider electron-proton deep inelastic scattering (DIS) [42, 43],

$$e^-(\ell) + p(P) \rightarrow e^-(\ell') + X, \quad (117)$$

via one-photon exchange. The amplitude for scattering off a single quark of flavor  $i$  and momentum  $k = xP$  is

$$\mathcal{M}_i = (-ie \bar{u}(\ell') \gamma^\mu u(\ell)) \frac{-ig_{\mu\nu}}{q^2} (ie_i \bar{u}(k+q) \gamma^\nu u(k)) \quad (118)$$

where  $q = \ell - \ell'$  and  $Q^2 = -q^2 > 0$ . Squaring

and summing over spins yields

$$|\mathcal{M}_i|^2 = \frac{e^4 e_i^2}{Q^4} L_{\mu\nu}(\ell, \ell') h^{\mu\nu}(k, q) \quad (119)$$

with the leptonic tensor

$$L_{\mu\nu} = \frac{1}{2} \sum_{\text{spins}} \bar{u}(\ell') \gamma_\mu u(\ell) \bar{u}(\ell) \gamma_\nu u(\ell') \quad (120)$$

and the partonic hadronic tensor

$$h^{\mu\nu}(k, q) = \frac{1}{2} \sum_{\text{spins}} \bar{u}(k) \gamma^\mu u(k+q) \bar{u}(k+q) \gamma^\nu u(k) \quad (121)$$

#### From Partonic to Proton Tensor

In the parton model one assumes the proton's hadronic tensor

$$W^{\mu\nu}(P, q) = \sum_i \int_0^1 dx f_i(x) h^{\mu\nu}(k = xP, q) \quad (122)$$

where  $f_i(x)$  is the probability to find a quark of flavour  $i$  carrying fraction  $x$  of the proton momentum. One then parametrizes

$$W^{\mu\nu} = \left( -g^{\mu\nu} + \frac{q^\mu q^\nu}{q^2} \right) F_1(x, Q^2) + \frac{(P^\mu - \frac{P \cdot q}{q^2} q^\mu)(P^\nu - \frac{P \cdot q}{q^2} q^\nu)}{P \cdot q} F_2(x, Q^2) \quad (123)$$

#### Structure Functions in the Parton Model

A straightforward calculation of  $h^{\mu\nu}$  yields the Born-level result

$$F_1(x, Q^2) = \frac{1}{2} \sum_i e_i^2 [f_i(x) + \bar{f}_i(x)], \quad (124)$$

$$F_2(x, Q^2) = x \sum_i e_i^2 [f_i(x) + \bar{f}_i(x)]$$

They satisfy the Callan-Gross relation  $2 \times F_1 = F_2$ , characteristic of spin-1/2 partons.

#### DIS Cross Section

The differential cross section in the laboratory frame is

$$\frac{d^2\sigma}{dxdy} = \frac{4\pi\alpha^2}{Q^4} \left[ (1 - y + \frac{y^2}{2}) F_2(x, Q^2) - \frac{y^2}{2} F_L(x, Q^2) \right] \quad (125)$$

where  $y = (P - q)/(P + \ell)$  and  $F_L = F_2 - 2x F_1 = 0$  at LO. Hence

$$\frac{d^2\sigma}{dxdy} = \frac{4\pi\alpha^2}{xyQ^2} \left[ 1 - y + \frac{y^2}{2} \right] x \sum_i e_i^2 [f_i(x) + \bar{f}_i(x)] \quad (126)$$

Thus, at leading order in the parton model

$$F_2(x, Q^2) = x \sum_i e_i^2 [q_i(x) + \bar{q}_i(x)] \quad (127)$$

and the measured DIS cross section directly probes the parton distribution functions  $f_i(x)$  weighted by the quark charges  $e_i^2$ .

#### 4.4 SUSY-Inversion Quark Charge Model with Whole Numbers

We introduce a multiplicative charge group  $M = \{+1, -1\}$  and a homomorphism

$$\phi : \{u, d\} \rightarrow M \quad (128)$$

defined by

$$\phi(u) = -1, \phi(d) = +1. \quad (129)$$

In the SUSY inversion model, the Down quark rest mass within the neutron is

$$4.84 \times 10^6 \text{ eV}/c^2 = 2.5617 \times 10^{-13} \text{ m} \quad (130)$$

and its reciprocal of

$$3.9036577 \times 10^{12} \text{ m}^{-1} \quad (131)$$

where

$$3.90365 \times 10^{12} \times 2.5617 \times 10^{-13} \text{ m} = 1$$

$$3.90365 \times 10^{12} \text{ m}^{-1} / 2.5617 \times 10^{-13} \text{ m} = 1.5238 \times 10^{25} \text{ m}^2$$

$$1 / 1.523 \times 10^{25} \text{ m}^2 = 6.5623 \times 10^{-26} \text{ m}^{-2} \quad (132)$$

The Balmer line electron transition  $n=3$  to  $n=2$  transition corresponds to 656.11 nm. This wavelength is also seen in the  $n=1$  position of the electron

$$5.7 \times 10^{27} / 8.6875 \times 10^{24} = 656.12 \text{ nm} \quad (133)$$

The aromatic ring radius in Planck lengths acts to frame the position of visible wavelengths of electromagnetism within the electron transition systems of the proton. The  $1 \times 10^{24} \text{ s}^2$  associated with the Charm quark generates 0.0656 and this has a  $\Delta$  of  $1 \times 10^5$  to the Down quark analysis indicating an involvement of the Strange quarks electric field decay.

The establishment of the photon wavelength in relationship to the electron location and the aromatic ring radius provides a framework in which the system is constrained by the geometric features and curvature of the aromatic ring. This structural framing of the electrons location and angular momentum provides the symmetry of the aromatic ring radius  $1.39 \times 10^{-10} \text{ m}$  with the age of the universe  $1.39 \times 10^{10} \text{ years}$ . It is within this holographic fractal relationship between the meter radius and age of the universe in years that the structure and function of spacetime geometry and the unification of GF and QM is proposed.

Within this geometric framing of the aromatic ring the Down quark's half-life of 888 s, and rest mass of  $4.84 \times 10^6 \text{ MeV}/c^2$  has a velocity of  $4.6698 \times 10^8 \text{ kJ/mole (m/s)}$ . This provides the following timings:  $5.49 \times 10^{-22} \text{ s}^2$  and  $1.44 \times 10^{-27} \text{ s}^3$  and  $s^2 = 789145.08 \text{ s}^2$  and the square root = 888.33838 s half-life. The second positional location:  $4.15 \times 10^{11} \text{ m}^2$ . The rest mass identifies the location where the particle resides at the point of the equilibrium (without interaction in its waveform). Inverse square law framing of the wavelength and its relationships with other wavelengths in differential velocities provides the basis for quantum gravitational calculations in  $\text{kJ/mole}$  (m/s) vs.  $\text{nm}$  for subatomic processes.

#### 4.5 First light timing and its boundary relationship to free neutron decay

Further exploration of the timings of first light in the universe at 380,000 years or  $1.1991888 \times 10^{13} \text{ s}$  provides a  $1 \times 10^{-6} \Delta \text{Charm}^{0.5} \text{ E}$  field decay between 888 s and light 888 location in the timing at 380,000 years. This bridge of symmetry between  $\text{DM} \rightarrow {}^{1/0} \text{H} \rightarrow {}^{1/1} \text{H}$  and matter and antimatter annihilation providing a compression system that forms light through maintaining conservation rules linked to  $\text{DE} \rightarrow {}^{3/2} \text{He}$  ( $\text{DE} \rightarrow {}^{1/1} \text{H} + {}^{2/1} \text{H} + {}^{3/2} \text{H} \rightarrow {}^{3/2} \text{He}$ ). The half-life temporal language can be modelled using SUSY inversion mapping language and  $\text{kJ/mole}$  (m/s) subatomic

modelling using 1 Planck length / second. The He-BEC modelling of DE and DM formation and the conservation of charge generation of isotopes from DE and DM will be presented elsewhere.

#### Single-Quark Charge Operators

Define the charge operator  $Q$  acting on quark states  $|u\rangle, |d\rangle$  by

$$\hat{Q}|u\rangle = \phi(u)|u\rangle = -|u\rangle, \quad \hat{Q}|d\rangle = \phi(d)|d\rangle = +|d\rangle \quad (134)$$

#### Multiplicative Baryon Charge

A baryon B composed of three quarks  $q_1, q_2, q_3 \in \{u, d\}$  is assigned the charge

$$Q^{\text{SUSY}}(B) = \phi(q_1)\phi(q_2)\phi(q_3) = \prod_{i=1}^3 \phi(q_i) \quad (135)$$

Equivalently, on the three-quark Fock state,

$$\begin{aligned} \hat{Q}|q_1 q_2 q_3\rangle &= (\hat{Q} \otimes \hat{Q} \otimes \hat{Q})|q_1 q_2 q_3\rangle \\ &= \left( \prod_{i=1}^3 \phi(q_i) \right) |q_1 q_2 q_3\rangle. \end{aligned} \quad (136)$$

Examples:

$$\begin{aligned} \text{Proton } (uud) : \quad Q^{\text{SUSY}}(p) &= \phi(u)\phi(u)\phi(d) \\ &= (-1) \times (-1) \\ &\times (+1) = +1, \end{aligned}$$

$$\begin{aligned} \text{Neutron } (udd) : \quad Q^{\text{SUSY}}(n) &= \phi(u)\phi(d)\phi(d) \\ &= (-1) \times (+1) \\ &\times (+1) = -1. \end{aligned} \quad (137)$$

#### Restoration of Neutron Neutrality

To recover the observed  $Q(n) = 0$ , one postulates an embedded positron state  $|e^+\rangle$  with charge +1. The full neutron state is

$$|n\rangle = |n_{\text{core}}\rangle \otimes |e^+\rangle \quad (138)$$

so that

$$\begin{aligned} \hat{Q}|n\rangle &= (\hat{Q}_{\text{core}} + \hat{Q}_{e^+})|n_{\text{core}}\rangle \otimes |e^+\rangle = (-1+1)|n\rangle \\ &= 0. \end{aligned} \quad (139)$$

#### Comments on Supersymmetry Inversion

One may view the map  $\phi$  as arising from an involutive "SUSY-inversion" operator  $S$  acting on the SM quark charges:

$$S : Q_q^{\text{SM}} \mapsto Q_q^{\text{rev}}, \quad S^2 = \mathbb{1} \quad (140)$$

with

$$S(+\frac{2}{3}) = -1, \quad S(-\frac{1}{3}) = +1 \quad (141)$$

This inversion swaps matter- and antimatter-like charge assignments at the quark level, and together with multiplicative composition restores full baryonic symmetry in the revised model.

## 5 Implications of Quark Charge Calculations Using the Supersymmetry Inversion Model

The implications of using the SUSY inversion model are significant for both particle physics and cosmology. By establishing baryonic symmetry through the pairing of protons with electrons (matter) and neutrons with positrons (antimatter), we can resolve the cosmological missing antimatter problem. This model suggests that the antimatter is not missing but is instead present in the atom in the form of positrons and neutrons, which are required to balance the negative charge of the neutrons. The revision of charges provides a logical framework to see the neutron as the antimatter particle to the protons matter. This model also has implications for the structure of the atom. The presence of positrons in the atom, particularly in the Bose-Einstein Condensate of helium-4, suggests that the atom is a more complex system than previously thought. The helium-4 atom, with its 16 fundamental particles, can be seen as a miniature universe, with a balanced number of matter and antimatter particles and a net overall charge of zero.

Furthermore, this model has implications for the initial state of the universe. The helium-4 Bose-Einstein Condensate could be the initial state of the universe, with a net charge of zero and a balanced number of matter and antimatter particles. This initial state would demonstrate superfluidity [44-51], with all particles in the same quantum state, which could explain the homogeneity of the cosmic microwave background radiation and the large initial singularity model enables a coherent initial structure that overcomes the horizon problem.

The SUSY inversion model also has implications for the unification of quantum mechanics (QM) and general relativity (GR). By using whole numbers and multiplication instead of fractions and addition, we can establish a more deterministic model of particle interactions, which could lead to a unified theory of quantum gravity based on the inverse square law using  $kJ/mole$  vs  $nm$ , we see a power law linked to quantum gravity. When plotting  $kJ/mole$  vs  $m$  we see a slope of  $1 \times 10^4$  which is shown above to be associated with the balance point in the charge generating system from the He-BEC modelling.

If positrons are present in atomic structures, a baryonic symmetrical state appears responsible for atomic stability. This framework suggests an inverse square law relationship between:

$$\begin{cases} \text{Matter pair: } (e^-, p^+) \\ \text{Antimatter pair: } (e^+, n^-) \end{cases} \quad (142)$$

where the radial distance between matter and antimatter components creates a balanced system analogous to a seesaw with a central pivot point. The alignment of the inverse square law theory with energy conservation can be expressed as:

$$\frac{k_{em}}{r_{e^-e^+}^2} = \frac{k_{strong}}{r_{pn}^2} \quad (143)$$

where  $k_{em}$  and  $k_{strong}$  represent electromagnetic and strong force constants respectively. The SUSY inversion model also reveals a fundamental relationship:

$$q_{\text{quark}} = q_{\text{electron}} \text{ (under charge parity)} \quad (144)$$

This symmetry carries profound implications for multiple physical phenomena, including isotope stability patterns,  $\beta$ -decay mechanisms, and the observed matter-antimatter asymmetry in the universe. The framework generates testable predictions spanning atomic and cosmological scales, unified through their common dependence on baryonic symmetry principles. Specifically, it suggests that the same underlying symmetry governs nuclear stability curves,  $\beta$ -transition probabilities ( $\Gamma_\beta$ ), and the matter-antimatter imbalance parameter ( $\eta \sim 6 \times 10^{-10}$ ), providing a bridge between quantum mechanical and cosmological phenomena. The He-BEC model maps cosmological composition to atomic theory to identify the structure of the singularity at the beginning of time.

## 6 Quark Charge and Supersymmetry Inversion in Beta Decay Systems

The SUSY inversion model also has implications for beta decay systems. In beta minus decay, a neutron decays into a proton, an electron, and an electron antineutrino. In the standard model, this is explained by the transformation of a down quark into an up quark, with the emission of a W boson, which then decays into an electron and an electron antineutrino.

In the SUSY inversion model, the neutron has a negative charge, which is balanced by a positron. During beta minus decay, the positively charged Down quark decays into a negatively charged electron, and the positron becomes integrated into the nucleus as a negatively charged Up quark. This can be represented as:

-Down quark (+1) decays into an electron (-1) and an electron antineutrino.

-Positron (+1) becomes integrated into the nucleus as an Up quark (-1).

This results in the transformation of the neutron (1 Up, 2

Down, 1 positron) into a proton (2 Up, 1 Down), with the emission of an electron and an electron antineutrino, maintaining charge conservation and conservation of angular momentum.

In beta plus decay, a proton decays into a neutron, a positron, and an electron neutrino. In the SUSY inversion model, the negatively charged Up quark decays into a positively charged positron, and the electron becomes integrated into the nucleus as a positively charged Down quark. This can be represented as:

-Up quark (-1) decays into a positron (+1) and an electron neutrino.

-Electron (-1) becomes integrated into the nucleus as a Down quark (+1).

This results in the transformation of the proton (2 Up, 1 Down) into a neutron (1 Up, 2 Down), with the emission of a positron and an electron neutrino, maintaining charge conservation. This model suggests that the entire atom is involved in beta decay, not just the nucleus, as the positrons and electrons in the atom's orbital layers play a role in the charge conservation process. This could have implications for our understanding of nuclear reactions and the stability of atoms.

### 6.1 Gamow-Teller Formalism for Neutron $\beta$ -Decay

We model free neutron decay

$$n \rightarrow p + e^- + \bar{\nu}_e \quad (145)$$

as an allowed Gamow-Teller transition [52, 53, 54, 55]. The total decay rate (inverse lifetime) is given by:

$$\lambda = \frac{\ln 2}{t_{1/2}} = \frac{G_F^2 |V_{ud}|^2}{2\pi^3 \hbar^7 c^5} (g_V^2 + 3g_A^2) \int_0^Q F(Z, E) p E (Q - E)^2 dE \quad (146)$$

where:

- $G_F$  = Fermi constant

- $V_{ud}$  = CKM element

- $g_V \approx 1$ ,  $g_A \approx 1.27$

- $F(Z, E)$  = Fermi function (for  $Z = 1$ )

- $p = \sqrt{E^2 - m_e^2}$ ,  $E$  = total electron energy

- $Q$  = endpoint energy (kinetic +  $m_e$ )

For a rough estimate we set  $F \approx 1$  and use the analytic approximation:

$$\int_0^Q p E (Q - E)^2 dE \approx \frac{Q^5}{30}, \quad (147)$$

so that:

$$\lambda \approx \frac{G_F^2 |V_{ud}|^2}{2\pi^3 \hbar^7 c^5} (1 + 3g_A^2) \frac{Q^5}{30}. \quad (148)$$

Inverting to solve for  $Q$  gives:

$$Q^5 = \frac{2\pi^3 \hbar^7 c^5 \ln 2}{30 G_F^2 |V_{ud}|^2 (1 + 3g_A^2) t_{1/2}} \equiv C / t_{1/2}. \quad (149)$$

Using the known neutron half-life  $t_{1/2} \approx 880$  s,  $GF = 1.166 \times 10^{-11}$  MeV $^{-2}$ ,  $V_{ud} \approx 0.974$ ,  $g_A = 1.27$ , we find numerically:

$$Q_{SM} \approx 0.782 \text{ MeV} \quad (150)$$

in perfect agreement with experiment.

### Shift by an Embedded Positron Binding Energy

If the neutron harbors a bound positron of binding energy  $B > 0$ , then the effective mass-difference available to the outgoing  $e^-$  and  $\bar{\nu}_e$  is increased by  $B$ . In other words,

$$Q_{rev} = Q_{SM} + B \quad (151)$$

The same Gamow-Teller formula then predicts larger endpoint:

$$Q_{rev}^5 = \frac{C}{t_{1/2}} \quad (152)$$

which implies

$$Q_{rev} = (C / t_{1/2})^{1/5} \quad (153)$$

so that

$$B = Q_{rev} - Q_{SM} \quad (154)$$

would be directly extractable from a precise measurement of the  $\beta$ -spectrum endpoint. In this model the existence of a nonzero  $B$  would shift the measured endpoint from its SM value of 0.782 MeV to  $0.782 + B$  MeV. A search for such a shift, at the few-keV level, provides a quantitative test of the "embedded positron" hypothesis.

## 7 More Features of the SUSY Inversion Model

The inverse square law's mathematical structure, fundamentally based on reciprocal relationships ( $1/x$ ), provides a natural framework for understanding charge inversion in supersymmetry models. This reciprocal operation, where multiplying a quantity by its inverse yield's unity ( $x \times 1/x = 1$ ), finds direct application in the SUSY inversion quark charge formalism. Here, quark charges can be represented as reciprocal pairs:

( ${}^{+1}/_1$ ,  ${}^{-1}/_1$ ,  ${}^{+1}/_{-1}$ ,  ${}^{-1}/_{-1}$ ), creating a unified mathematical language that bridges fractional and integer charge representations through bosonic statistics. The relationships

between positron and electron within the atomic structure of s orbitals can then be explored using this combination of frameworks.

The E-fields and B-fields interacting at  $90^\circ$  to generate  $c^2$  which is framed in terms of a SUSY inversion geometry corresponding to  $E/M = c^2$ . This framing of bosons having no mass and an overall charge state equal to zero. The arrows indicating opposite charges causing attractions and like charges repulsion. The concave surface is negatively charged, and its angular momentum is counterclockwise [cc] and the convex surface is positive, and the angular momentum is clockwise [c]. The proposed model establishes a mathematical framework with four 90-degree quadrants containing charge pairs:

$$\begin{cases} 1 \times -1 = -1 & \text{(electron)} \\ -1 \times -1 = +1 & \text{(positron)} \\ -1 \times 1 = -1 & \text{(electron)} \\ 1 \times 1 = +1 & \text{(positron)} \end{cases} \quad (155)$$

This configuration suggests two electrons (-1) and two positrons (+1) within the s-orbital layer, with geometric alignment:

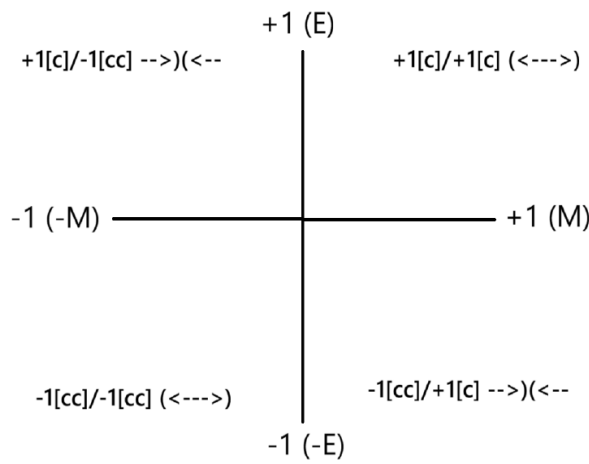


**Fig. 4:** Combination of fractions and whole numbers for the Boson and Fermion statistics for Bose Einstein Condensates. Angular momentum [c] - clockwise, [cc] - counterclockwise,  $\rightarrow$ ) $\leftarrow$  compression and blue shift,  $\leftarrow$ ) $\rightarrow$  expansion and red shift. Concave -) negative and convex +) positive.

$$\sin(90^\circ) = 1 \text{ (perfect orthogonal alignment)} \quad (156)$$

During  $\beta$ -decay processes, quark transformations occur through:

$$\begin{aligned} \beta^- \text{ decay: } & n \rightarrow p + e^- + \bar{\nu}_e \\ & \text{(Down quark} \rightarrow \text{Up quark)} \\ \beta^+ \text{ decay: } & p \rightarrow n + e^+ + \nu_e \\ & \text{(Up quark} \rightarrow \text{Down quark)} \end{aligned} \quad (157)$$

The characteristic timescales reveal fundamental limitations:

**Table 1:** Temporal scales in nuclear processes

Process	Timescale
W/Z boson mediation	$1 \times 10^{-25}$ s
Current attosecond technology	$1 \times 10^{-18}$ s
LHC collision analysis	$1 \times 10^{-27}$ s

The nuclear event horizon analogy draws striking parallels between atomic nuclei and black hole physics, suggesting three key phenomena: (1) information confinement mechanisms analogous to black hole thermodynamics, (2) a seven-order-of-magnitude disparity ( $1 \times 10^7$ ) between observable timescales in nuclear processes versus current attosecond measurement capabilities, and (3) the utility of high-energy collisions as probes of cosmological-scale conditions. These theoretical insights are driving cutting-edge experimental approaches, including attosecond spectroscopy for resolving electron dynamics at  $1 \times 10^{-18}$  s timescales, ultra-relativistic collisions at the LHC achieving energies of 13TeV, and advanced quantum chromodynamics (QCD) simulations bridging non-perturbative regimes. Together, these efforts aim to unravel the quantum gravitational signatures potentially encoded in nuclear structure and dynamics.

The SUSY inversion framework for quark charge calculations, through its inherent baryonic symmetry, suggests an alternative cosmological mechanism where particle interactions strictly conserve energy via transformation rather than creation or destruction. This model proposes that the universe maintains energy conservation through precise matter-antimatter transformations ( $\phi \leftrightarrow \phi$ ) at the quark level, with the SUSY inversion (SI) operator ensuring that all energy states satisfy:

$$\sum_i E_i^{\text{matter}} = \sum_j E_j^{\text{antimatter}} \quad \text{for } t \in (-\infty, +\infty) \quad (158)$$

The mathematical structure reveals that apparent particle creation/annihilation processes are actually energy-state transformations.

In this way the conservation of energy can be used to explore the processes involved in beta decay where either an electron or a positron is released from the nucleus of the atom rather than from its orbital layer. This would suggest that the whole atom is involved in its rearrangement, giving rise to an alternative explanation for the beta decay system. It is proposed that the quark of opposite charge is responsible for the origin of the decayed electron and antineutrino or positron and the neutrino in the beta decay system as outlined in Figure 5.

The SUSY inversion model proposes a novel  $\beta^-$  decay pathway:

$$d^+ \rightarrow u^- + e^- + \tilde{V}_e \text{ (with positron } e^+ \text{ absorbed)} \quad (159)$$

in the table given in Figure 6.

This process maintains energy conservation through:

- Down quark ( $d^+$ )  $\rightarrow$  Up quark ( $u^-$ ) charge inversion
- Electron ( $e^-$ ) emission via W boson mediation
- Positron ( $e^+$ ) incorporation into nuclear structure

The model predicts stability when:

$$\begin{cases} N_p = N_n \\ N_{e^-} = N_{e^+} \end{cases} \quad (160)$$

where deviation from this matter-antimatter balance correlates with instability. The SUSY inversion model also predicts doubled orbital capacities:

**Table 2:** Orbital occupancy comparison

Model	s	p	d	f
Standard	2	6	10	14
Supersymmetry	4	12	20	28

The square law progression emerges as:

$$2^2 = 4 \quad (\text{s}) \quad (161)$$

$$4^2 = 16 = 12_p + 4_s \quad (162)$$

$$6^2 = 36 = 20_d + 12_p + 4_s \quad (163)$$

$$8^2 = 64 = 28_f + 20_d + 12_p + 4_s \quad (164)$$

The model suggests that conventional quark charge calculations may represent broken symmetry states rather than fundamental properties. The ability to model atoms and their potential properties may be a function of number theory. The central location within the atom provides a potential reference point and this is identical for all atoms. Having an internal frame of reference provides for a relativistic feature of atomic theory aligned with Einstein geometry.

The periodic table of elements has 7s orbital layers and the following pyramidal square law arrangement. There are 7s orbital layers, there are 6p orbital layers, 4d orbital layers and 2f orbital layers. Each s orbital containing 4 particles in the SUSY inversion model. Here  $7 \times 4 = 28$ , that corresponds to one f orbital layer. There appears to be processes within atomic theory that have set forth a framework that generates a stable atomic structure based on the inverse square law theory. This would enable a single-atom framework to be established and explored to ascertain if single atoms can be modelled and facilitate the exploration and explanation of the parameters operating in atoms and the cosmos. A number theory for the periodic table of elements is outlined

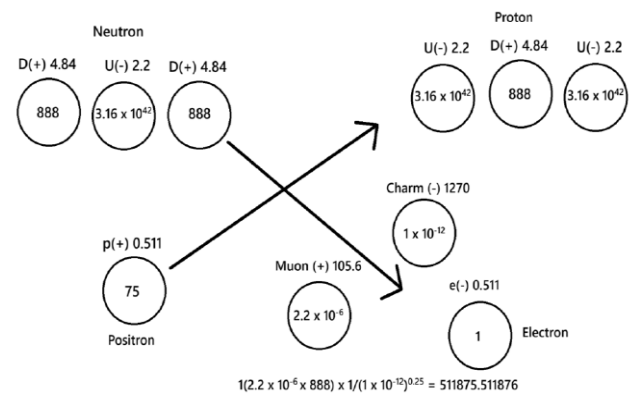


**Fig. 5:** SUSY inversion beta minus decay process.

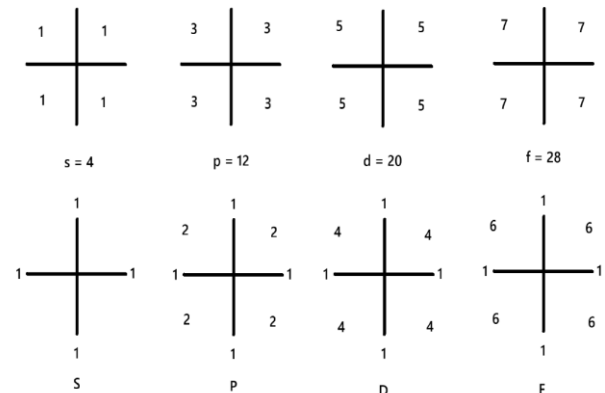


**Fig. 6:** Inverse square law theoretical modelling of atomic structure of positron and electron pairing associated with s, p, d, and f orbitals in atoms of the periodic table.

Orbital layer	identity	$28(p)(-N)(-e)(+p)$	72	80	56	
He-BEC	He-BEC	$s(4+2e+2e^+)$	$p(12+6e+6p^+)$	$d(20+10e+10p^+)$	$f(28+14e+10p^+)$	Numbers
DE	DE	$4 \rightarrow \dots$	$12 \rightarrow \dots$	$20 \rightarrow \dots$	$28 \rightarrow \dots$	$16(+8)$
DM	DM	$4(-2+2=0)$	$12(-6+6=0)$	$20(-10+10=0)$	$28(-14+14=0)$	$DE(4) \rightarrow 1/0 H(2)$
Photon	X	$X(0=2-2)$				$DM(4) \rightarrow 1/0 H(2)$
-1	1/0H	$4H(0)(0)(1)(+1)$				$c^2 = E/M$
1	1/1H	$4H(+1)(0)(-1)(0)$				1s
2	2/1H	$8D(+1)(1)(-1)(+1)$				1s2s
3	3/1H	$12D(+1)(-2)(-1)(+2)$				1s2s3s
4	4/1H	$16D(+1)(-3)(-1)(+3)$				1s2s3s4s
5	5/1H	$20D(+1)(-4)(-1)(+4)$				1s2s3s4s5s
6	6/1H	$24D(+1)(-5)(-1)(+5)$				1s2s3s4s5s6s
7	7/1H	$28D(+1)(-6)(-1)(+6)$				1s2s3s4s5s6s7s
8	8He(0) 2/2He	$8He(+2)(0)(-2)(0)$				1s2s
9	12He(1) 3/2He	$12He(+2)(-1)(-2)(+1)$				1s2s3s
10	16He(2) 4/2He	$16He(+2)(-2)(-2)(+2)$	$16He(+2)(-2)$			1s2p
11	20He(3) 5/2He	$20He(+2)(-3)(-2)(+3)$	$20He(+2)(-2)$			1s2s2p
12	24He(4) 6/2He	$24He(+2)(-4)(-2)(+4)$	$24He(+2)(-2)$			1s2s3s2p
13	28He(5) 7/2He	$28He(+2)(-5)(-2)(+5)$	$28He(+2)(-2)$			1s2s3s4s2p
14	32He(6) 8/2He	$32He(+2)(-6)(-2)(+6)$	$32He(+2)(-2)$			1s2s3s4s5s2p
15	36He(7) 9/2He	$36He(+2)(-7)(-2)(+7)$	$36He(+2)(-2)$			1s2s3s4s5s6s2p
16	40He(8) 10/2He	$40He(+2)(-8)(-2)(+8)$	$40He(+2)(-2)$			1s2s3s4s5s6s7s2p
17	12Li(0) 3/3Li	$12Li(+3)(0)(-3)(0)$				1s2s3s
18	16Li(1) 4/3Li	$16Li(+3)(-1)(-3)(+1)$	$16Li(+3)(-3)$			1s2p
19	20Li(2) 5/3Li	$20Li(+3)(-2)(-3)(+2)$	$20Li(+3)(-3)$			1s2s2p

**Fig. 7:** The initial three elements and their isotopes of the Periodic Table of Elements According to the SUSY Inversion Model

There is a specific biological locus where SUSY inversion is applicable. It is within this location where the symmetry between the age of the universe and radius of the aromatic ring are correlated. This is the location where the subatomic pathways associated with the standard model of particle physics bridge the boundary between stable atomic forms and DE and DM boundaries of the universe. It appears that unstable atoms act as a go between language and form the basis of a type of communication between the atomic universe and the spatial and temporal universe. Therefore, LENR and isotope systems can be considered to be important in a biological phenomenon connected to the aromatic ring. Processes associated with the proton and its interaction within the aromatic ring are proposed to be critical in the evolution of biological energetics linking unstable atom processes with cosmological compositional information. Further details correlating this relationship will be presented elsewhere.

### 7.1 Zero Charge State?

There appears to be useful information obtained in understanding why the periodic table of elements is formed in the way it has. By utilizing Baryonic symmetry and equal parts matter and antimatter as proposed by the SUSY inversion modelling. This could shed some light onto the cosmological processes operating within the universe. The idea that matter and antimatter are made in equal amounts during the birth of the universe (cosmic inflation), provides the basis that the entire universe originated from a zero state where all of the energy present was essentially at an identical level. The cosmic microwave background (CMB) provides evidence for such a hypothesis. If we assume that the universe arose from nothing and describe the features of nothing that give rise to everything then the structure of nothing and the early universe can be described. In this baryonic symmetry model the nothingness of the early universe can be described in terms of a balance of matter and antimatter giving a mathematical language off negative charge equal to the amount of positive charge. This could account for the overall zero charge state of the primordial universe. The implications of baryonic symmetry obtained from quark charge calculations therefore provide the basis of understanding that the early universe did not contain charged particles.

## 8 Integration with the He-BEC Isotropic Singularity Framework

### Initial He-BEC State

The Universe begins in a homogeneous superfluid of Helium-4 described by a condensate wavefunction

$$\Psi(\mathbf{r}, t) = \sqrt{n_0} e^{-i\mu t/\hbar}, \quad \mu = 0. \quad (165)$$

Define the total charge and effective baryon number operators

$$\hat{Q} = \hat{Q}_{\text{core}} + \hat{Q}_{e+}, \quad \hat{B}_{\text{eff}} = \hat{B}_{\text{core}} - \hat{L}_{e+} \quad (166)$$

By hypothesis, the BEC carries no net charge and no net effective baryon number:

$$\hat{Q}|\Psi_{\text{BEC}}\rangle = 0, \quad \hat{B}_{\text{eff}}|\Psi_{\text{BEC}}\rangle = 0. \quad (167)$$

### SUSY-Inversion Core and Embedded Positron

Each neutron in the BEC is modelled as

$$|n\rangle = |n_{\text{core}}\rangle \otimes |e^+\rangle, \quad (168)$$

with

$$\hat{Q}_{\text{core}}|n_{\text{core}}\rangle = -1|n_{\text{core}}\rangle, \quad \hat{Q}_{e+}|e^+\rangle = +1|e^+\rangle, \quad (169)$$

$$\hat{B}_{\text{core}}|n_{\text{core}}\rangle = +1|n_{\text{core}}\rangle, \quad \hat{L}_{e+}|e^+\rangle = -1|e^+\rangle. \quad (170)$$

Hence

$$\hat{Q}|n\rangle = (-1+1)|n\rangle = 0, \quad \hat{B}_{\text{eff}}|n\rangle = (1-1)|n\rangle = 0. \quad (171)$$

### Emission and Partition of Constituents

As the BEC “decays” (drives inflation and cosmic expansion), it breaks up into

$$|\Psi(t)\rangle = \sum_{N_\alpha, N_e, N_{e+}} C_{N_\alpha, N_e, N_{e+}} |N_\alpha; N_e; N_{e+}\rangle, \quad (172)$$

with the total number constraint  $N_\alpha + N_e + N_{e+} = N_0$ . Each Fock state still satisfies

$$\hat{Q}|N_\alpha, N_e, N_{e+}\rangle = 0, \quad \hat{B}_{\text{eff}}|N_\alpha, N_e, N_{e+}\rangle = 0. \quad (173)$$

### Cosmic Energy Densities

Identify

$$\begin{aligned} \rho_{\text{DE}} &= \frac{N_\alpha m_\alpha c^2}{V}, & \rho_{\text{DM}} &= \frac{(N_e + N_{e+}) m_e c^2}{V} \\ \rho_b &= \frac{N_p m_p c^2}{V}, \end{aligned} \quad (174)$$

where  $N_p$  is the small remnant of free protons (each also  $\hat{B}_{\text{eff}} = +1$ ). Define the critical density  $\rho_c = 3H_0^2/(8\pi G)$  and cosmic fractions

$$\begin{aligned} \Omega_i &= \frac{\rho_i}{\rho_c} \implies \Omega_{\text{DE}} \approx 0.68, \Omega_{\text{DM}} \approx 0.27, \Omega_b \\ &\approx 0.05. \end{aligned} \quad (175)$$

### Resolution of the Baryon Asymmetry

The observed baryon-asymmetry parameter normally is [56, 57, 58, 59],

$$\eta_B = \frac{n_B - n_{\bar{B}}}{n_\gamma} \quad (176)$$

where  $n_B = n_p + n_n$ . In our framework, each neutron carries no effective baryon number, so the true effective asymmetry is

$$\eta_B^{\text{eff}} = \frac{n_{B_{\text{free}}} - n_{\bar{B}_{\text{free}}} - (n_{e_{\text{hid}}^+} - n_{e_{\text{hid}}^-})}{n_\gamma} = 0 \quad (177)$$

The apparent excess of free baryons ( $n_p$ ) is exactly offset by the hidden positrons ( $n_{e+_{\text{hid}}} = n_n$ ), thus restoring zero net effective baryon number in the Universe.

This unified formalism shows how a SUSY-inverted, whole-number quark-charge model with embedded positrons, when embedded in a primordial He-4 BEC singularity, naturally yields:

- a zero-charge, zero-effective-baryon-number initial state,
- Emission of neutral  $\alpha$ -particles driving dark energy cosmic inflation at  $2.9907 \times 10^9$  m/s based on the wavelength of  $4 \times 10^{-14}$  m.
- Liberation and collapse of leptons driving dark matter at the inverse square velocity of 54687.29285 m/s from  $4 \times 10^{-14}$  m to  $1.6 \times 10^{-35}$  m, a  $\Delta = 4 \times 10^{-22}$  m.
- To DE = 75% (12/16), DM = 25% (4/16), and M = 0%. Then, life of neutral alpha particle DE and DM of  $1 \times 10^{18}$  s is DE and decay = 7.26% after  $4.36 \times 10^{17}$  s ( $13.8 \times 10^9$  years) giving 67.74% DE, 27.42% DM, and 4.84% M.
- R = c, and Charge parity maintained through  $\text{DE} \rightarrow {}^3/2 \text{ He}$  and  $\text{DM} \rightarrow {}^1/0 \text{ H}$ .
- Energy conservation through  $\sqrt{v}/v = 1/\sqrt{v}$  and  $(\sqrt{v})^8 = v^4$
- and a vanishing effective baryon asymmetry without explicit B-violation.

## 9 Effective Baryon Number and the Baryon Asymmetry

### Standard Definition of Baryon Asymmetry

The usual baryon-asymmetry parameter is

$$\eta_B = \frac{n_B - n_{\bar{B}}}{n_\gamma} \quad (178)$$

where  $n_B$  ( $n_B$ ) is the number density of free baryons (antibaryons) and  $n_\gamma$  the photon density. Observationally,

$$\eta_B \sim 6 \times 10^{-10} \quad (179)$$

$1/v + 1/v = 6.6873976 \times 10^{-10}$  s/m (1/kJ/mole) based on  $\Delta 4 \times 10^{-14}$  m in the He-BEC singularity.

### Core and Embedded States

In the SUSY-inversion model, each neutron is a bound state

$$|n\rangle = |n_{\text{core}}\rangle \otimes |e^+\rangle \quad (180)$$

with

$$\begin{aligned} Q(n_{\text{core}}) &= -1, & Q(e^+) &= +1, & B(n_{\text{core}}) &= +1 \\ L(e^+) &= -1. \end{aligned} \quad (181)$$

Here B is quark-number/3 and L the usual lepton number.

$K_e = 8.99 \times 10^9$  where

$$1/v = 3.3436988 \times 10^{-10} \text{ s/m} / 3 = 1.1145663 \text{ E} - 10 \text{ s/m}$$

$$1/1.1145663 \times 10^{-10} = 8972100000 \text{ m/s.}$$

$$8972100000 \text{ m/s} / 8.99 \times 10^9 = 0.99800889877$$

### Effective Baryon-Number Operator

Define an effective baryon-number operator

$$\hat{B}_{\text{eff}} = \hat{B}_{\text{core}} - \hat{L}_{e^+} \quad (182)$$

such that on the neutron state

$$\begin{aligned} \hat{B}_{\text{eff}} |n\rangle &= (\hat{B}_{\text{core}} - \hat{L}_{e^+}) |n_{\text{core}}\rangle \otimes |e^+\rangle \\ &= (1 - 1) |n\rangle = 0. \end{aligned} \quad (183)$$

Likewise for an antineutron (if it existed).

### Total Effective Asymmetry

Let  $n_B$  free be the density of free baryons (protons, neutrons) and  $n_{e+_{\text{hid}}}$  the density of hidden (embedded) positrons. Then the net effective baryon asymmetry is

$$\eta_B^{\text{eff}} = \frac{n_{B_{\text{free}}} - n_{\bar{B}_{\text{free}}} - (n_{e_{\text{hid}}^+} - n_{e_{\text{hid}}^-})}{n_\gamma} \quad (184)$$

But in our model

$$n_{\bar{B}_{\text{free}}} = 0, \quad n_{e_{\text{hid}}^-} = 0, \quad n_{e_{\text{hid}}^+} = n_n \quad (185)$$

and

$$n_{B_{\text{free}}} = n_p + n_n = n_p + n_{e_{\text{hid}}^+} \quad (186)$$

Hence

$$\eta_B^{\text{eff}} = \frac{(n_p + n_{e_{\text{hid}}^+}) - 0 - (n_{e_{\text{hid}}^+} - 0)}{n_\gamma} = \frac{n_p}{n_\gamma} \quad (187)$$

If one measures only

$$\eta_B \equiv \frac{n_p + n_n}{n_\gamma} \quad (188)$$

one finds an “excess” of baryons. But the true effective

asymmetry, including the hidden positrons, is

$$\eta_B^{\text{eff}} = \frac{n_p}{n_\gamma} - \frac{n_{e_{\text{hid}}^+}}{n_\gamma} + \frac{n_{e_{\text{hid}}^+}}{n_\gamma} = 0 \quad (189)$$

By enlarging the definition of “baryon asymmetry” to include the embedded positrons as carrying negative effective baryon number (via

$$\hat{B}_{\text{eff}} = \hat{B} - \hat{L} \quad (190)$$

one finds that the Universe started—and remains—in a state of zero effective baryon asymmetry. The observed excess of free baryons is exactly balanced by the hidden anti-leptons in neutrons. In this sense the model “solves” the missing antimatter problem and the baryon asymmetry without invoking new B-violating interactions.

The alpha particle emission process from the Helium Bose Einstein condensate singularity provides an energy conservation process that provides the initial generation of DE and DM in a 3:1 ratio. The  $1 \times 10^{18} \text{ s}^{1/2}$  life aligns with cosmic inflation of  $1 \times 10^{27} \text{ m}$  and  $1 \times 10^{-36} \text{ s}$  in inverse square law framing the universe process of inflation with DE and compression with DM. The decay timings aligning atomic theory 4.84% M and cosmological composition of 67.74% DE and 27.42% DM at the current timing of  $1.38 \times 10^{10}$  years.

## 10 Conclusion & Discussion

Atoms are among the smallest structures in the universe, and unlocking the principles that govern their behaviour could revolutionize modern science and technology. A refined atomic model holds the promise of enabling advances such as atomic computation and novel quantum phenomena like tunnelling and entanglement—features that could one day make instant communication via entangled states a reality. However, our ability to probe atomic structure is fundamentally limited by current temporal and spatial measurement technologies. These constraints have contributed to enduring theoretical divisions between quantum mechanics and general relativity, as well as to gaps within the Standard Model of particle physics.

Presently, our dominant scientific frameworks fall short in explaining several key phenomena. Among the most pressing are the identity and origin of the universe’s missing baryonic antimatter—predicted by the Big Bang and hot nucleosynthesis models—and the enigmatic nature of dark matter and dark energy, which collectively account for approximately 95% of the universe’s total composition [60, 61]. Though we cannot measure these components directly, their existence is inferred from cosmological observations such as the effects of cosmic inflation and the gravitational behaviour of galaxies over the 13.8-billion-year history of the universe.

Scientific progress demands fertile intellectual ground—an environment where bold, new ideas can take root and flourish. In this spirit, the development of a new atomic model that incorporates positrons into atomic structure represents a conceptual seedling: the emergence of baryonic symmetry. Could this symmetry provide the foundation for a transformation of our understanding of matter and antimatter? Quantum mechanics has brought us far over the past century, offering profound insights into wave-particle duality, the collapse of the wavefunction, and the inherent uncertainty of quantum states. Yet, it keeps us anchored to the past—bound by measurement and constrained by the very limits of what we can observe.

The SUSY inversion model of quark charge calculations introduces a novel framework grounded in the inverse square law, offering a more deterministic and predictive approach to atomic theory. Early indications suggest that the inclusion of positrons not only restores baryonic symmetry but also aligns with a more universal principle—where matter and antimatter are produced in equal amounts. Their mutual annihilation yields photons, massless and chargeless carriers of energy, and one of the four fundamental forces of nature in atomic structure, further tying into Einstein’s profound equation:  $E = mc^2$  and its rearrangement to  $c^2 = E/M$  and the right-hand rule of electromagnetism where / represents 90° and the intersection of E and M fields. In this geometry of light (no mass and no charge), the M represents magnetism rather than mass in the revised form. The rearrangement corresponds to the tunnelling process where matter is formed through quantum tunnelling and the formed product has both charge and mass generated through asymmetry of three quarks and one orbital particle.

To fully grasp the implications of mass-energy equivalence and the role of light in atomic processes, a deeper theoretical understanding is required. The SUSY inversion model may provide new insights into the electromagnetic interactions that underlie atomic structure and, potentially, into the elusive goal of unifying quantum mechanics with gravity. Ongoing investigations aim to determine whether this model can address the many unresolved questions of modern physics. Should the presence of positrons in atoms and the symmetry they introduce be confirmed, it could represent the foundation of a new scientific discipline, and a crucial step toward a comprehensive theory of quantum gravity.

Scientific models are meant to evolve, and if an existing model cannot withstand scrutiny, then its foundation, especially if built solely on reductionist measurement, must be reconsidered. Such a foundation cannot serve as a lasting basis for knowledge or its meaningful application for humanity.

A new atomic model is emerging, grounded in baryonic symmetry through the inclusion of positrons within atomic structures. This framework, based on SUSY inversion quark charge calculations, employs charge parity between positrons and electrons to propose the existence of a negatively charged neutron as the antimatter partner of

opposite charge to the proton within the nucleus of the atom. By replacing fractional charges with whole numbers and adopting multiplicative logic, the SUSY inversion model introduces positrons into atomic theory. This innovation enables the neutralization of the negatively charged neutron by pairing it with a positively charged positron. This approach not only explains why the neutron is more massive than the proton, but also accounts for phenomena such as beta-plus decay (where a positron is emitted) and the inherent instability of free neutrons is determined through the half-life timings of 888 s and 75 s linking the  $DM \rightarrow {}^1/{}_0 H \rightarrow {}^1/{}_1 H$  process generating the asymmetry observed through the temporal half-life differences and atomic instability based on  $uu = d$  and  $dd \neq u$ . Here  $d \rightarrow uu$  at 888 s and the timings of events are linked to antimatter decay processes.

The process of  $uu \rightarrow d$  is therefore proposed to be a way that stored antimatter is used biologically to time duplication structure through symmetry in biological living systems. This appears to be connected to healing and regeneration as well as atomic doublings. This symmetry replication system offers an underlying subatomic mechanism for cell division. Such quantum processes within biological living systems offer biologists a unique opportunity to see both chiral structure and their decay timings associated with biological systems evolving from the processes operational within the proton. A greater depth of information is now available to biologists looking for a logic-based model for the interpretation of quantum coherent living systems. The inclusion of atomic instability and antimatter as energy features within atoms offers new information to help address the difficult question “What is Life”.

Together, these insights offer compelling evidence for the SUSY inversion as an alternative model to the Standard Model of quark charge calculations. This has opened the door to a deeper and more symmetric understanding of atomic structure and the processes associated with the dynamics of living systems.

## 11 Appendix

### 11.1 Standard Model Limitations

Quarks in the Standard Model interact via all four fundamental forces, with charges calculated additively [6]:

$$\text{Proton (2 Up, 1 Down): } +2/3 + 2/3 - 1/3 = +1 \quad (191)$$

$$\text{Neutron (1 Up, 2 Down): } +2/3 - 1/3 - 1/3 = 0 \quad (192)$$

The neutron's higher mass (939.565 MeV/c<sup>2</sup> vs. 938.272 MeV/c<sup>2</sup>) and the absence of antimatter remain unresolved [6]. Fractional charges complicate baryonic symmetry, and the hot Big Bang model struggles with JWST data [4].

Here are some profound limitations of the standard model that might be worth looking at:

#### Neutrino Masses

In the SM, neutrinos are strictly massless because no

renormalizable gauge-invariant mass term exists:

$$\mathcal{L}_\nu^{\text{SM}} \supset 0 \quad (193)$$

One can write only a dimension-5 Weinberg operator,

$$\mathcal{O}_5 = \frac{c_{ij}}{\Lambda} (L_i \tilde{\phi})(L_j \tilde{\phi}), \quad \tilde{\phi} = i\sigma_2 \phi^* \quad (194)$$

which after EWSB ( $\langle \phi \rangle = v/\sqrt{2}$ ) gives  $m_\nu \sim c v^2/\Lambda$ , but  $\mathcal{O}_5$  is not part of the renormalizable SM Lagrangian.

#### Dark Matter

The SM has no neutral, colourless, stable particle with the right relic density. A minimal extension might introduce a singlet fermion  $\chi$ :

$$\mathcal{L}_\chi = \bar{\chi}(i\partial - m_\chi)\chi + y_\chi \bar{\chi}\chi \phi^\dagger \phi \quad (\chi \notin \text{SM}) \quad (195)$$

#### Baryon Asymmetry

The SM contains CP violation via the CKM phase, quantified by the Jarlskog invariant

$$J = \text{Im}[V_{ud} V_{cs} V_{us}^* V_{cd}^*] \sim 3 \times 10^{-5} \quad (196)$$

and an electroweak phase transition that is not strongly first order. Together they fail to generate the observed  $\eta_B \approx 6 \times 10^{-10}$  through electroweak baryogenesis.

#### Hierarchy (Naturalness) Problem

Quantum corrections to the Higgs mass are quadratically divergent:

$$\delta m_h^2 \sim \frac{\Lambda^2}{16\pi^2} \left( 6\lambda + \frac{9}{4}g^2 + \frac{3}{4}g'^2 - 6y_t^2 \right) \quad (197)$$

To keep  $m_h \approx 125$  GeV with a cutoff  $\Lambda \gg$  TeV requires severe fine-tuning.

#### Strong CP Problem

QCD allows a CP-violating term

$$\mathcal{L}_\theta = \theta \frac{g_s^2}{32\pi^2} G_{\mu\nu}^a \tilde{G}^{a\mu\nu}, \quad \tilde{G}^{a\mu\nu} = \frac{1}{2}\epsilon^{\mu\nu\rho\sigma} G_{\rho\sigma}^a \quad (198)$$

yet experiments constrain  $\theta \lesssim 10^{-10}$  with no explanation in the SM.

#### Gauge Coupling Unification

The one-loop beta-functions

$$\mu \frac{dg_i}{d\mu} = \frac{b_i}{16\pi^2} g_i^3, \quad b_i = \left\{ \frac{41}{10}, -\frac{19}{6}, -7 \right\} \quad (199)$$

do not lead to a single unification scale without extra fields.

#### Absence of Gravity

The SM Lagrangian

$$\mathcal{L}_{\text{SM}} = \mathcal{L}_{\text{gauge}} + \mathcal{L}_{\text{fermion}} + \mathcal{L}_{\text{Higgs}} + \mathcal{L}_{\text{Yukawa}} \quad (200)$$

contains no dynamical metric  $g_{\mu\nu}$  or Einstein-Hilbert term and so cannot describe gravitational interactions.

#### Cosmological Constant Problem

The vacuum energy from EWSB and QCD condensates,

$$\rho_{\text{vac}} \sim \langle V(\phi) \rangle + \mathcal{O}(\Lambda_{\text{QCD}}^4) \geq (10^2 \text{ GeV})^4 \quad (201)$$

overshoots the observed  $\rho \Lambda \approx (10^{-3} \text{ eV})^4$  by some 55 orders of magnitude.

## References

[1] Gell-Mann, M. (1964). A Schematic Model of Baryons and Mesons. *Physics Letters*, 214-215. doi:10.1016/S0031-9163(64)92001-3.

[2] Zweig, G. (1964). An SU(3) Model for Strong Interaction Symmetry and its Breaking: II. CERN Document Server, CERN-TH-412.

[3] NASA. (2015). Universe 101: Our Universe. Retrieved from <https://svs.gsfc.nasa.gov/12307>.

[4] Colin, J., Mohayee, R., Rameez, M., & Sarkar, S. (2019). Evidence for anisotropy of cosmic acceleration. *Astronomy & Astrophysics*, 631, L13.

[5] Weinberg, S. (1989). The cosmological constant problem. *Reviews of Modern Physics*, 61(1), 1-23.

[6] Nave, R. (2008). Quarks. HyperPhysics. Georgia State University, Department of Physics and Astronomy.

[7] Helium-4. (2025). Wikipedia. Retrieved from <https://en.wikipedia.org/wiki/Helium-4>.

[8] Redd, N. T. (2013). What is dark energy? Space.com.

[9] J. Parra, R. Poberezhniuk, V. Koch, C. Ratti, and V. Vovchenko, “Evidence for freezeout of charge fluctuations in the quark-gluon plasma at the LHC,” arXiv:2504.02085 [hep-ph], Apr. 2025.

[10] D. Kotlorz and O. V. Teryaev, “Charge sum rules for quark fragmentation functions” arXiv:2502.00733 [hep-ph], Feb. 2025.

[11] Y.-B. Liu, B. Hu, and C.-Z. Li, “Single production of vectorlike quarks with charge 5/3 at the 14 TeV LHC,” *Nucl. Phys. B*, vol. 1007, p. 116667, Oct. 2024, arXiv:2402.01248 [hep-ph].

[12] H. Dahiya, S. Dutt, A. Kumar, and M. Randhawa, “Axial-vector charges of the spin  $1/2^+$  and spin  $3/2^+$  light and charmed baryons in the SU(4) chiral quark constituent model,” *Eur. Phys. J. Plus*, vol. 138, no. 5, p. 441, May 2023, arXiv:2305.02630 [hep-ph].

[13] A. Chaudhuri and M. Yu. Khlopov, “Charge asymmetry of new stable quarks in baryon asymmetrical Universe,” arXiv:2110.09973 [hep-ph], Oct. 2021.

[14] L. Du, “Hydrodynamic description of the baryon-charged quark-gluon plasma,” arXiv:2107.08368 [nucl-th], Jul. 2021.

[15] A. Dumitru, H. M'antysaari, and R. Paatelainen, “Cubic color charge correlator in a proton made of three quarks and a gluon,” *Phys. Rev. D*, vol. 105, no. 3, p. 036007, Feb. 2022, arXiv:2106.12623 [hep-ph].

[16] Y. Uesugi, H. Yamashiro, T. Suehara, T. Yoshioka, and K. Kawagoe, “Quark charge identification for e+e- to q-q study,” arXiv:1902.05242 [physics], Feb. 2019.

[17] ATLAS Collaboration, “Measurement of the charge asymmetry in highly boosted top quark pair production in  $\sqrt{s} = 8 \text{ TeV}$  pp collision data collected by the ATLAS experiment,” *Phys. Lett. B*, vol. 756, pp. 52-71, May 2016, arXiv:1512.06092 [hep-ex].

[18] ATLAS Collaboration, “Measurement of the charge asymmetry in top-quark pair production in the lepton-plus-jets final state in pp collision data at  $\sqrt{s} = 8 \text{ TeV}$  with the ATLAS detector,” *Eur. Phys. J. C*, vol. 76, no. 2, p. 87, Feb. 2016, arXiv:1509.02358 [hep-ex].

[19] CMS Collaboration, “Measurement of the charge asymmetry in top quark pair production in pp collisions at  $\sqrt{s} = 8 \text{ TeV}$  using a template method,” *Phys. Rev. D*, vol. 93, no. 3, p. 034014, Feb. 2016, arXiv:1508.03862 [hep-ex].

[20] C. W. Murphy, “Bottom-Quark Forward-Backward and Charge Asymmetries at Hadron Colliders,” *Phys. Rev. D*, vol. 92, no. 5, p. 054003, Sep. 2015, arXiv:1504.02493 [hep-ph].

[21] P. Scior, S. R. Edwards, and L. von Smekal, “Fractional Charge and Confinement of Quarks,” arXiv:1311.3854 [hep-lat], Nov. 2013.

[22] A. Ray and S. Sanyal, “Baryon inhomogeneities in a charged quark gluon plasma,” *Phys. Lett. B*, vol. 726, no. 1-3, pp. 83-87, Oct. 2013, arXiv:1309.1236 [hep-ph].

[23] M. A. Faessler, “Weinberg Angle and Integer Electric Charges of Quarks”, arXiv:1308.5900 [hep-ph], Aug. 2013.

[24] P. Rau, J. Steinheimer, S. Schramm, and H. Stöcker, “Conserved Charge Fluctuations in a Chiral Hadronic Model including Hadrons and Quarks,” arXiv:1308.4319 [hep-ph], Sep. 2013.

[25] H. Schiff, “Charge without charge in quarks,” arXiv:1308.1341 [physics], Aug. 2013.

[26] I. C. Cloet, C. D. Roberts, and A.W. Thomas, “Revealing dressed-quarks via the proton's charge distribution,” arXiv:1304.0855 [nuclth], Apr. 2013.

[27] P. E. Shanahan, A. W. Thomas, and R. D. Young, “Charge symmetry breaking from a chiral extrapolation of moments of quark distribution functions,” arXiv:1303.4806 [nuclth], Mar. 2013.

[28] I. V. Frolov, M. V. Martynov, and A. D. Smirnov, “The chiral color symmetry of quarks and G' -boson contributions to charge asymmetry in  $t\bar{t}$ -production at the LHC and Tevatron,” arXiv:1302.5316 [hep-ph], Mar. 2013.

[29] S. Berge and S. Westhoff, “Top-Quark Charge Asymmetry

with a Jet Handle,” arXiv:1208.4104 [hep-ph], Nov. 2012.

[30] S. Pratt, “Identifying the Charge Carriers of the Quark-Gluon Plasma,” arXiv:1203.4578 [nucl-th], Mar. 2012.

[31] G. C. Nayak, “General Form of Color Charge of the Quark,” arXiv:1201.2672 [hep-ph], May 2013.

[32] J. H. Kuhn and G. Rodrigo, “Charge asymmetries of top quarks at hadron colliders revisited,” arXiv:1109.6830 [hep-ph], Dec. 2011.

[33] S. Pratt, “General Charge Balance Functions, A Tool for Studying the Chemical Evolution of the Quark-Gluon Plasma,” arXiv:1109.3647 [nucl-th], Jan. 2012.

[34] S. R. Edwards, A. Sternbeck, and L. von Smekal, “Exploring a hidden symmetry with electrically charged quarks,” arXiv:1012.0768 [hep-lat], Dec. 2010.

[35] G. Bregar and N. S. M. Borstnik, “New experimental data for the quarks mixing matrix are in better agreement with the spin-charge-family theory predictions” arXiv:1412.5866 [hep-ph], Jun. 2015.

[36] N. Yamanaka, “Quark scalar, axial and tensor charges in the Schwinger-Dyson formalism” arXiv:1412.5794 [hep-ph], Dec. 2014.

[37] U. De Sanctis, “Top quark charge asymmetry measurements with ATLAS detector” arXiv:1411.3544 [hep-ex], Nov. 2014.

[38] S.-Q. Wang, X.-G. Wu, Z.-G. Si, and S. J. Brodsky, “Application of the Principle of Maximum Conformality to the Top-Quark Charge Asymmetry at the LHC” arXiv:1410.1607 [hep-ph], Nov. 2014.

[39] D0 Collaboration, “Measurement of the Electric Charge of the Top Quark in  $t\bar{t}$  Events,” arXiv:1407.4837 [hep-ex], Sep. 2014.

[40] M. Malaver, “Quark star model with charge distributions,” arXiv:1407.1936 [gr-qc], Jul. 2014.

[41] R. Aaij et al., “First measurement of the charge asymmetry in beauty-quark pair production at a hadron collider” arXiv:1406.4789 [hep-ex], Sep. 2014.

[42] M. E. Peskin, D. V. Shroeder, “An Introduction To Quantum Field Theory” CRC Press (1995).

[43] Matthew D. Schwartz, “Quantum Field Theory and the Standard Model”, Cambridge University Press (2013).

[44] M. Fedi, A Superfluid Theory of Everything?, HAL Id: hal-01312579 (2016).

[45] Veronika E Hubeny, Shiraz Minwalla, Mukund Rangamani, The fluid/gravity correspondence, arXiv:1107.5780 [hep-th] (2011).

[46] Veronika E Hubeny, The fluid/gravity correspondence: a new perspective on the membrane paradigm, Classical and Quantum Gravity, 28 (11) 114007 (2011). HAL Id: hal-00705158

[47] N. Afshordi, Gravitational Aether and the thermodynamic solution to the cosmological constant problem, arXiv:0807.2639 [astroph] (2008).

[48] G. E. Volovik, “The Universe in a Helium Droplet,” vol. 117, 2003.

[49] K. Huang, “A Superfluid Universe”, (2016). <https://doi.org/10.1142/10249>

[50] K. Huang, “Dark Energy and Dark Matter in a Superfluid Universe”, Int. J. Mod. Phys. A, 28 1330049 (2013). arXiv:1309.5707 [gr-qc]

[51] S. Azmi, A. Pushp. “Aether Integration” Preprints 2021050491 (2021). doi: 10.20944/preprints202105.0491.v1

[52] Gamow, G. and Teller, E. Phys. Rev. 49, 895 (1936).

[53] Y. Fujita, “Detailed study of Gamow-Teller transitions: The impact on astro and nuclear-structure physics”, Nuclear Physics A, vol. 805 (2008).

[54] Muna Al-Harby, Bassam A. Shehadeh, “Review of Gamow-Teller and Fermi Transition Strength Functions”, arXiv:2211.02164 [nucl-th] (2022).

[55] Stewart D. Bloom, “On the Prevalence of the Gamow-Teller Transition”, Book chapter pp 15-37 in “Energy in Physics, War and Peace” Editors: Hans Mark and Lowell Wood.

[56] John D. Barrow, “Baryon asymmetry with cosmological asymmetries”, Monthly Notices of the Royal Astronomical Society, 189 (1), (1979).

[57] A. Riotto; M. Trodden, “Recent progress in baryogenesis”, Annual Review of Nuclear and Particle Science 49: 46 (1999). arXiv:hep-ph/9901362

[58] Canetti, L.; Drewes, M.; Shaposhnikov, M. “Matter and Antimatter in the Universe”, New J. Phys. 14 (9): 095012 (2012). arXiv:1204.4186

[59] S.M. Boucenna, S. Morisi, “Theories relating baryon asymmetry and dark matter: a Mini review”, Front. Physics 1:33 (2013). arXiv:1310.1904 [hep-ph]

[60] E. Oks, “Brief Review of Recent Advances in Understanding Dark Matter and Dark Energy”, New Astronomy Reviews, 93, 101632 (2021). arXiv:2111.00363 [astroph. CO]

[61] V. Sahni, “Dark Matter and Dark Energy, Lect.NotesPhys, 653 : 141-180, (2004). arXiv:astro-ph/0403324